Cerebral blood flow variability from morning to evening and after sleep deprivation

An arterial spin labeling study

Marie Strømstad

Master of Philosophy in Psychology
Cognitive Neuroscience

UNIVERSITY OF OSLO

May 2018

Cerebral blood flow variability from morning to evening and after sleep deprivation: an arterial spin labeling study

© Marie Strømstad

2018

Cerebral blood flow variability from morning to evening and after sleep deprivation: an arterial spin labeling study

Marie Strømstad

http://www.duo.uio.no/

Trykk: Reprosentralen, Universitetet i Oslo

Summary

Name of author: Marie Strømstad

Title of thesis: Cerebral blood flow variability from morning to evening and after sleep deprivation: an arterial spin labeling study

Supervisor: Inge Groote

Co-supervisor: Torbjørn Elvsåshagen

Author statement: The thesis is part of a larger research project and served as a pilot for the project. The author, a fellow master student and our supervisor Inge Groote carried out the collection of the data.

Abstract:

Even though sleep is universal and a prominent aspect of our life, the function of sleep and the underlying neurobiological mechanisms are not completely understood. The importance of sleep can be seen after sleep deprivation, as lack of sleep is associated with impaired attentional and cognitive functioning. Considering the role of the thalamus in the arousal system and cortical network, this subcortical structure seems particularly sensitive to sleep deprivation. The current study aimed to investigate thalamic cerebral blood flow (CBF) variability from morning to evening and after 24 and 32 hours of sleep deprivation using pseudo-continuous arterial spin labeling (PCASL) perfusion magnetic resonance imaging. Ten healthy participants were scanned on four occasions; in the morning, in the evening, the next morning and the afternoon. The PCASL-analysis and quantification of CBF were performed in nordicICE, and CBF-values were extracted from subject-specific thalamus masks. Although we found large mean decreases after 24 hours (22.2 %) and 32 hours (19.3%) of sleep deprivation, this did not reach significance. One explanation of the lack significant results might be our small sample size accompanied by a conservative multiple comparison correction. Further investigation is needed to explore these interesting trends towards changes in thalamic CBF from morning to evening and after sleep deprivation using larger sample sizes.

Acknowledgements

I would like to thank my supervisors Dr. Inge Groote and co-supervisor Dr. Torbjørn Elvsåshagen for allowing me to be a part of a very interesting project and for giving me great opportunities throughout the year to learn and grow as a researcher.

Especially thanks to Inge for giving many feedbacks on my drafts, and for your availability, encouragements, expertise in MRI methodology, which has been truly valuable. Thank you to Prof. Atle Bjørnerud for additional help on the analysis in nordicICE.

Furthermore, I would like to thank my fellow master student, Irene Voldsbekk, for the collaboration in preparations of the study and data collection.

A special thanks to all of the participants that agreed to be a part of the experiment, allowing us to investigate your sleep deprived brains.

Table of Contents

1 INTRODUCTION

Sleep consumes about a third of our lives, with an average healthy sleep duration of approximately 7 hours (Watson et al., 2015). Sleep problems are common and affecting about one third of the population (Ohayon, 2011). Sleep problems are associated with increased risk of accidents (Åkerstedt, Philip, Capelli, & Kecklund, 2011) and a range of diseases (Grandner, Hale, Moore, & Patel, 2010). Furthermore, sleep is necessary for optimal attentional and cognitive performance (Buxton et al., 2012). Interestingly, sleep deprivation has been shown to have an acute antidepressant effect in 50-60 % of patients with major depressive disorder, with relapse after recovery sleep (Wolf et al., 2016).

Even though sleep is universal and a prominent aspect of our life, the function of sleep and the underlying neurobiological mechanisms are not completely understood. In the rapidly growing sleep literature, several theories and hypotheses have emerged, which will be reviewed as well as the neurobiology of the sleep-wake cycle, including the ascending reticular activating system, which is involved in modulating alertness and cortical arousal levels (Saper, Scammell, & Lu, 2005).

One method of studying the function of sleep is through sleep deprivation studies, where individuals are deprived from sleeping in an extensive period to investigate its effect on the neuronal mechanisms and cognitive functions. The thalamus, which plays a crucial role in the activating system and modulates cortical arousal which is important for wakefulness (Lim & Dinges, 2008), is believed to be particularly sensitive to sleep deprivation.

One method to investigate alteration in neural baseline activity is by using a perfusion neuroimaging method called arterial spin labeling (ASL), which measures cerebral blood flow (CBF) (Alsop et al., 2015). This method was employed in the current study and will be further described. The main goal of this thesis is to contribute to the ongoing research on sleep deprivation, by investigating thalamic CBF variability from morning to evening and after sleep deprivation.

1.1 The two-process model

The two-process model is the dominating sleep regulation theory (Daan, Beersma, & Borbely, 1984). This model indicates that the sleep-wake cycle is regulated by a circadian and a homeostatic process, and together they determine the timing of sleep and wakefulness. The circadian rhythm ("process C") is in part regulated by an internal biological clock driven by the suprachiasmatic nucleus (SCN) in the anterior hypothalamus (Moore, 2007) and running on a 24-hour cycle. More specifically, there is a three-stage pathway from the SCN to the subparaventricular zone, a region just in front of and below the SCN, and then to the dorsomedial nucleus of the hypothalamus, which in turn transmits circadian information to cell groups involved in sleep and wake regulation. This includes gamma-amino-butyric acid (GABA)ergic projections to the ventrolateral (VLPO) and median optic nucleus (MnPO), glutamatergic projections to lateral hypothalamic area (Saper, Lu, Chou, & Gooley, 2005) and glutamatergic and GABAergic inputs to the paraventricular nucleus of the thalamus (Colavito, Tesoriero, Wirtu, Grassi-Zucconi, & Bentivoglio, 2015). The circadian signal promotes wakefulness throughout the day and is dependent on the environmental light-dark cycle. Animal studies report that lesions to the SCN result in loss of circadian rhythm in their sleep-wake cycle (e.g., Liu, Zhang, Xu, Huang, & Qu, 2012).

The homeostatic process ("process S"), representing a homeostatic sleep drive or sleep pressure, builds up during wakefulness and declines during sleep (Daan et al., 1984). In other words, the longer you are awake, the stronger the pressure to sleep becomes, and the longer you are asleep, the more the pressure to sleep decreases. Increases in sleep pressure are associated with decreases in cognitive performance and alertness (Gaggioni, Maquet, Schmidt, Dijk, & Vandewalle, 2014). Sleep or wake occurs when process S is above or below a threshold, respectively, and the threshold is dependent on the circadian signal (Daan et al., 1984). The circadian alerting signal is strongest in the evening (approximately between 20:00 and 22:00) to counteract the increase in sleep pressure, preventing us from falling asleep, and at night transmits circadian information to sleep-promoting neurons (Gaggioni et al., 2014). The mechanism underlying process S and its anatomical substrate has not yet been fully identified. It has been suggested that a region in the hypothalamus, the MnPO, is responsive to sleep pressure as GABAergic neurons in this region are activated during sleep deprivation prior to sleep onset (Schwartz & Kilduff, 2015). Additionally, findings from animal studies suggest that sleep pressure results from increases in sleep-promoting substances, such as

adenosine, which increases throughout the day in the basal forebrain and binds to receptors in sleep-promoting areas, including the MnPO, to promote sleep (Schwartz & Kilduff, 2015). However, the underlying mechanism of process S is still not fully understood.

1.2 Synaptic homeostasis hypothesis

One influential hypothesis suggests that process S reflects synaptic homeostasis (Tononi & Cirelli, 2003, 2006). During wakefulness, learning and experience lead to an increase in the number and strength of synapses, and this overall synaptic weight decreases during sleep until it reaches a baseline level when sleep ends (Figure 1). According to the hypothesis, sleep is needed to downscale the synaptic weight after a day of wake to reserve energy and space resources, prevent synaptic overload and to preserve the efficiency of integrating and encoding information. Specifically, this downscaling involves a proportional decrease of overall synaptic strength. Thus, the strongest synapses survive and the weakest synapses are downscaled below a minimum strength and removed. Therefore, the function of sleep is to improve the signal-to-noise ratio (SNR) by renormalizing the overall synaptic strength and preserving the most stable memory traces.

Supporting evidence largely derives from electrophysiological and molecular findings in animal studies, demonstrating wake-dependent increases and sleep-dependent decreases in various markers of synaptic strength, such as number or size of synapses in flies (Bushey, Tononi, & Cirelli, 2011) and levels of GluR1-containing α-amino-3-hydroxy-5-methyl-4-isoxazolepropionic acid receptors in the cortex and hippocampus of rats (Vyazovskiy, Cirelli, Pfister-Genskow, Faraguna, & Tononi, 2008). There is further supporting findings from human studies, indirectly investigating the synaptic homeostasis. For example, a learning task involving specific brain areas produced a local increase in slow-wave activity, an electrophysiological marker for synaptic downscaling, during the following night of sleep (Huber, Felice Ghilardi, Massimini, & Tononi, 2004).

Synaptic activity, including action potentials and postsynaptic potentials, is responsible for most of the brain energy metabolism (Attwell & Laughlin, 2001). Therefore, as synaptic strength increases throughout the day, brain metabolism should also increase, and similarly decrease during sleep. This has been found in mice, in which wakefulness was associated with increased levels of cerebral metabolic rate (CMR), which decreased after sleep (Vyazovskiy, Cirelli, Tononi, & Tobler, 2008). However, there are conflicting findings from human studies.

Region-specific increases in CMR during wakefulness has been found in hypothalamic and brainstem structures (Buysse et al., 2004) and another study found a trend towards CMR increase from morning to afternoon (Bartlett et al., 1988). However, other studies have not found diurnal increases (Hodkinson et al., 2014; Shannon et al., 2013), but one study found decreases in CMR during sleep (Boyle et al., 1994).

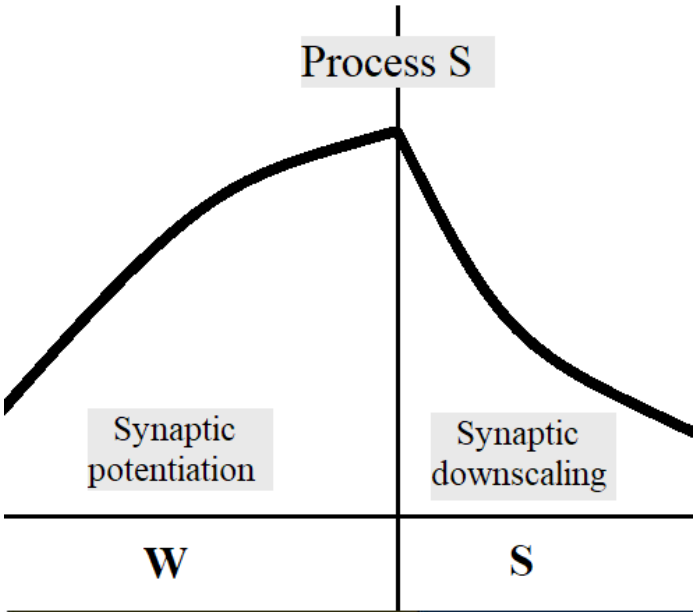

Figure 1. Synaptic homeostasis hypothesis: wakefulness (W) is associated with net synaptic potentiation, in which the overall synaptic strength increases. During sleep (S), the synaptic weight is downscaled until it reaches a baseline level. Adapted from Tononi and Cirelli (2006).

1.3 Neurobiology of the sleep-wake cycle

As previously mentioned, the SCN transmits circadian information to cell groups involved in sleep/wake regulation. Cell groups that promote wakefulness are found in the brainstem, hypothalamus and basal forebrain, and this brain circuitry is called the reticular activation system (RAS) (Saper, Scammell, et al., 2005). These wake-promoting cell groups activate the thalamus and the cerebral cortex through two pathways (Figure 2). The thalamus (including thalamic relay neurons, reticular nucleus and intralaminar/midline nuclei) is mainly activated by cholinergic cell groups in the brainstem, including neurons in the upper pons, pedunculopontine (PPT) and laterodorsal tegmental nuclei (LDT). This activation enables the thalamus to relay information from sensory inputs before transmitting the information to the

cerebral cortex, which in turn activates the cortex where the information is further processed through the thalamocortical circuitry.

The cerebral cortex is also activated directly through a second pathway by neurons in monoaminergic cell groups in the upper brainstem, including the serotoninergic dorsal and median raphe nuclei and noradrenergic locus coeruleus (LC), and by neurons in the hypothalamus, including tuberomammillary nucleus (TMN) containing histamine, and dopaminergic neurons adjacent to the dorsal raphe nucleus. The cerebral cortex also receives input from peptidergic neurons in the lateral hypothalamus, containing orexin and melanin-concentrating hormone (MCH), as well as from basal forebrain neurons containing acetylcholine or GABA (Saper, Scammell, et al., 2005).

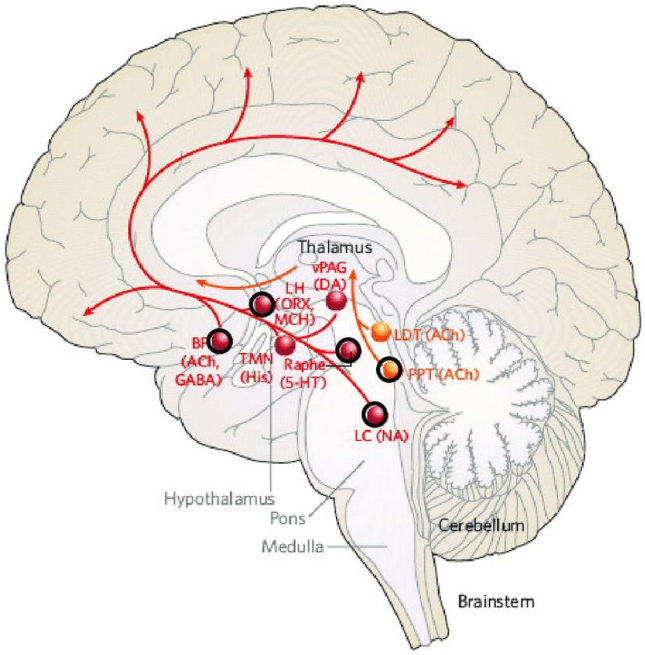

Figure 2. The reticular activation system (RAS) (Saper, Scammell, et al., 2005). Thalamus is activated through the first pathway (orange) by cholinergic (ACh) neurons in the brainstem (PPT, LDT), and the cortex then receives the thalamic input. The second pathway (red) activates the cerebral cortex from serotoninergic (5-HT) and noradrenergic (NA) neurons in the upper brainstem (LC and Raphe), histaminergic (His) and dopaminergic (DA) in the hypothalamus, orexin (ORX) neurons in the lateral hypothalamus (LH) and GABAergic and cholinergic neurons in the basal forebrain (BF). Reproduced from Saper, Scammel and Lu (2005).

Neurons in the MnPO and the VLPO are sleep-promoting neurons. Increased activity in the MnPO neurons is seen during sleep deprivation and prior to sleep onset (Hsieh et al., 2011), suggesting a role in increasing sleep pressure, and VLPO neurons are active during sleep

(Saper, Fuller, Pedersen, Lu, & Scammell, 2010). The sleep-promoting substance, adenosine, which builds up throughout wakefulness, binds to receptors on the MnPN and VLPO to promote sleep (Schwartz & Kilduff, 2015). There is a mutual inhibitory mechanism that underlie the transition between wake and sleep Activation of MnPO and VLPO neurons results in a release of the inhibitory neurotransmitters galanin and GABA, which inhibit the wake-promoting neurons, and sleep is promoted. The monoaminergic arousal cell groups in turn inhibit the VLPO and MnPO neurons to promote wakefulness again, with contributions from orexin neurons, which strengthen the arousal systems.

1.4 Sleep deprivation

Sleep deprivation can potentially lead to numerous negative neurobehavioral consequences, such as impaired attention and working memory, and other cognitive deficits (Lim & Dinges, 2010). These deficits have been associated with attention and control network areas such as the thalamus, basal ganglia and frontal and parietal cortices (Ma, Dinges, Basner, & Rao, 2015). Total sleep deprivation, as defined the complete lack of sleep for a certain period, has also been found to have an antidepressant effect in depressive patients (Benedetti & Colombo, 2011), associated with changes in brain metabolism in specific brain regions such as the medial prefrontal cortex and the ventral anterior cingulate cortex (Wu et al., 1999). Patients with depression have been associated with impaired synaptic plasticity (Wolf et al., 2016) and disturbed circadian rhythms (McClung, 2007). It is therefore of great importance to investigate the neurobiological effects of sleep deprivation.

According to the synaptic homeostasis hypothesis, wakefulness is associated with an increase in total synaptic weight, and the function of sleep is to downscale overall synaptic weight. Thus, sleep deprivation might lead to synaptic overload and failure. Indeed, neuronal “tiredness” has been observed in rats during sleep deprivation, in which neurons "go offline” and exhibit slow-wave activity (Vyazovskiy et al., 2011). The cognitive deficits seen after sleep deprivation thus may reflect decreased neuronal excitability and altered synaptic activity in the attention and control networks.

As the RAS plays a crucial role in maintaining a healthy sleep-wake cycle, sleep deprivation would probably affect this system. Generally, sleep deprivation is associated with continued activation in this wake-promoting system (Longordo, Kopp, & Lüthi, 2009). Additionally, sleep-active neurons in the VLPO and MnPO has been shown to be activated

and associated with increased waking discharge in response to sleep deprivation (Alam, Kumar, McGinty, Alam, & Szymusiak, 2014). As mentioned, the thalamus is activated by cholinergic neurons in the brainstem (Saper, Scammell, et al., 2005). During sleep deprivation, adenosine increases and inhibit the activity of cholinergic neurons, which in turn alter thalamocortical arousal (Strecker et al., 2000). Thalamic activity is also influenced by orexins, in which orexins specifically modulate activity in the intralaminar/midline thalamic nuclei (Govindaiah & Cox, 2006). In response to sleep deprivation, the effect of orexin decreases due to the inhibitory effect of noradrenaline, (Grivel et al., 2005), which again alters the thalamic activity. Taken together, the thalamic nuclei seems to be particularly sensitive to sleep deprivation.

1.5 The thalamus

1.5.1 Thalamic structure

The thalamus is a subcortical structure of grey matter and comprises multiple subnuclei which have different functional specializations to process different kinds of information with distinct anatomical connections to the cortex and other subcortical structures (Sherman, 2007). The thalamus can be divided into relay nuclei, the reticular nucleus and intralaminar/midline nuclei. The thalamic relay nuclei can be further separated into first and higher order relay neurons, based on their inputs and outputs (Sherman, 2007). The first order relays receive sensory information directly from sensory receptors and transmit the information to the associated areas in the cortex where it is processed. For example, the lateral geniculate thalamic nuclei receive inputs from the optic nerve and outputs to the primary visual cortex (Guillery & Sherman, 2002). The higher order relays receive information after being processed by the cortex and are believed to be the link in a corticothalamocortical circuitry, which consists of looped neural pathways that continuously process information to and from thalamus and the cortex and facilitate corticocortical communication (Sherman, 2007). Examples of higher-order relays are the anterior thalamic nuclei, which are connected to the hippocampus and contribute to encoding and recollective memory processes (Van der Werf, Jolles, Witter, & Uylings, 2003), and the pulvinar nuclei involved with visual attention due to their connections to the superior colliculus and parietal cortex (Fama & Sullivan,

2015). The reticular nucleus of the thalamus, which is located between the thalamic relay neurons and the cerebral cortex, does not project to the cerebral cortex but instead modulates the thalamocortical activity by activating or inhibiting the thalamic relay neurons (Pinault, 2004). The intralaminar/midline thalamic nuclei have long been considered to be part of the "non-specific nuclei" due to their diffuse and non-specific projections to different areas of the cortex (Van der Werf, Witter, & Groenewegen, 2002). However, different regions in this nuclei have been associated with specific brain functions (e.g., cognitive, sensory and motor functions), and their overall function is to mediate cortical arousal to promote awareness with strong inputs from the brainstem (Van der Werf et al., 2002). The paraventricular thalamic nucleus (PVT), which is part of the intralaminar/midline thalamic nuclei, has connections to mood-regulating structures, such as the nucleus accumens and the amygdala (Hsu, Kirouac, Zubieta, & Bhatnagar, 2014). Interestingly, a recent study also demonstrated a link between depression and the PVT, in which mice expressed human-like depressive symptoms when signals from the PVT to other parts of the brain was blocked (Kasahara et al., 2016). Furthermore, it has lately received much attention in its involvement with circadian timing and sleep/wake regulation and it has been suggested that the PVT reflects a meeting point for the interaction between thalamic and hypothalamic mechanisms (Colavito et al., 2015). As described previously, the SCN projects information about the circadian timing to the subparaventricular zone and the dorsomedial nucleus of the hypothalamus, which then transmit circadian information to other cell groups. The PVT is one of the cell groups receiving circadian information, and it is suggested that PVT neurons may transmit circadian information to the medial prefrontal cortex and nucleus accumbens (Colavito et al., 2015).

1.5.2 Sleep deprivation and the thalamus

Previous findings of altered thalamic activity following sleep deprivation is consistent with the role of the thalamus in cerebral activation and alertness. For example, Shao et al. (2013) found that 36 hours of sleep deprivation altered the thalamocortical functional connectivity. Furthermore, studies using positron-emission tomography (PET) have reported a reduced absolute glucose metabolism in the thalamus, basal ganglia and frontal lobe after about 32 hours of sleep deprivation (Wu et al., 1991; Wu et al., 2006). Thomas et al. (2000) found decreases in regional CMRglu after 24 hours of sleep deprivation in several cortical and subcortical structures, with the greatest reductions in the thalamus and prefrontal and

posterior parietal cortices. In a later study, the same areas were found to decrease even further after 48 and 72 hours of sleep deprivation (Thomas et al., 2003).

However, there are also some conflicting findings regarding the thalamic activation following sleep deprivation. Poudel, Innes and Jones (2012) found no change thalamic CBF after sleep restriction, only CBF decreases in the frontoparietal cortex in the most tired participants. Increases in thalamic activity have also been reported after sleep deprivation (e.g. Tomasi et al., 2009). One argument is that the increased activity in the thalamus after sleep deprivation may reflect a greater effort to compensate for the decreased frontoparietal attentional network seen after sleep deprivation, as a negative correlation has been reported between thalamic activity and parietal and prefrontal activity (Tomasi et al., 2009). However, most of the research reporting this increased thalamic activity are from functional magnetic resonance imaging (fMRI) studies using blood-oxygen-level dependent imaging (BOLD) and reflects task-specific temporarily increases and not thalamic baseline levels. Further investigation is needed to asses the effects of sleep deprivation on overall thalamic activation at baseline level.

In addition to neuroimaging data, the effects of sleep deprivation can also be seen by using behavioural measures, such as self-reported sleepiness questionnaires and objective measurements, such as a psychomotor vigilance test. This task is a sensitive measure of sustained attention, often used in sleep deprivation studies. Sustained attention, or vigilance, refers to the ability to ignore irrelevant stimuli, be consistently attentive and alert during repetitive activity (Lim & Dinges, 2008). The task measures the reactions times to visual stimuli presented at random onsets, and it has been demonstrated that sleep deprivation causes a slowing of reaction times and increased error rates (Lim & Dinges, 2008). Consistent with the thalamus being associated with sustained attention (Lim & Dinges, 2008), research has shown that decreased performance is linked with decreased CBF in the thalamus (Paus et al., 1997), and resting CBF activity can predict subsequent performance, with greater performance associated with higher resting CBF in the thalamus (Lim et al., 2010).

1.6 Arterial Spin Labeling (ASL)

Perfusion can be defined as the physiological process of the delivery of nutrients, such as oxygen and glucose, to the capillary bed (Chappell, MacIntosh, & Okell, 2017). Changes in

perfusion can be an indication of, for example, an increase in demands for nutrients during neuronal activation.

Perfusion weighted imaging allows for an investigation of the perfusion of tissue by blood. ASL is a participant-friendly, non-invasive method to investigate perfusion *in-vivo* in the brain. Unlike PET or MRI-based perfusion techniques such as dynamic susceptibility contrast (DSC) and dynamic contrast-enhancement (DCE), ASL requires no contrast agent injections, as the blood-borne tracer is generated by the magnetic resonance imaging (MRI) scanner itself. As seen in Figure 3, ASL produces an image by labelling arterial blood water with a radiofrequency pulse (RF) in the neck, before the blood-water enters the region of interested in the brain where it is imaged (Grade et al., 2015). More specifically, the radiofrequency pulse causes the magnetization of the water molecules to be inverted, and this creates a tracer in the blood-water. After the labelling is done, there is a post-labelling delay (PLD), in which the labelled blood water travels from the neck to the region of interest (ROI) and the labelled image is acquired. Another image without labelling - the control image - is then acquired, and a subtraction of the label-control pair produce a perfusion-weighted image, which scales directly to CBF.

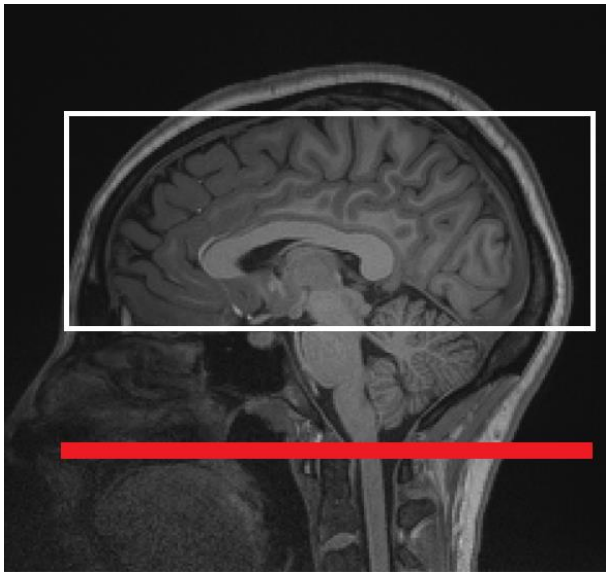

Figure 3. Arterial blood water is labelled (red line) before entering the region of interest in the brain (white box), which is then imaged.

The main disadvantage of using ASL is the SNR, which is inherently low since the labelled blood water comprise only about 1-2 % of the total arterial blood water (Chappell et al., 2017). Careful selection of labelling methods and appropriate parameters is important to improve the SNR.

Labelling methods

There are several different labelling methods, including pulsed ASL (PASL), continuous ASL (CASL) and pseudo-continuous ASL (PCASL) (Alsop et al., 2015). While the labelling phase is very brief (10-20 milliseconds) in PASL, contributing to poor SNR, the CASL method has a long labelling duration, typically 1-3 seconds, created by external hardware that is difficult to implement in practice. In PCASL, a series of 1000 or more brief RF pulses are used to label. PCASL is the recommended labelling method as it takes advantage of both the high SNR from CASL and the higher labelling efficiency in PASL (Alsop et al., 2015). The PCASL method is fairly easy to implement on modern MRI scanners.

ASL parameters and background suppression

To acquire good quality ASL data, the PLD is the most critical parameter, and it should be correctly adjusted. If the PLD is too short, the labelled blood-water will not have had enough time to enter the region of interest. If the delay is too long, the labelled water will to a larger extent decay before it reaches the ROI, as the label disappears after a few seconds (Chappell et al., 2017). It is recommended that the PLD in PCASL is 1.8 seconds for healthy, young individuals (Alsop et al., 2015), however, the optimal PLD depends on the blood velocity (Grade et al., 2015). For example, narrow arteries and poor cardiac output leads to slower velocity, and would ideally require longer PLD (Zaharchuk, 2014). Another parameter worth mentioning is voxel size, as spatial resolution affects the SNR. SNR decreases with increases in resolution (smaller voxel size) (Chappell et al., 2017). However, low spatial resolution (large voxel size) will obviously make it difficult to identify in which specific brain region the perfusion signals occurs. This will also contribute to the partial volume effect, in which voxels contains both white and grey matter (Grade et al., 2015). MRI scanners with a field strength of 3 Tesla (3T), voxel sizes of $4mm^3$ are seen as reasonable (Chappell et al., 2017).

To improve SNR, background suppression is also recommended. Background suppression refers to the suppression of signals from the brain tissue itself, so that when the pairwise subtraction of the label and control images is done, the difference reflects the perfusion alone

(Chappell et al., 2017). One method in which background suppression can be achieved is by using a saturation pulse, which removes any static tissue signal within the imaging region at the time of image acquisition (Alsop et al., 2015).

CBF quantification

ASL can be used to quantify perfusion and this is achieved using an established kinetic model (Buxton et al., 1998), which is expressed as:

$$CBF = \frac{6000 \cdot \lambda \cdot (SI_{control} - SI_{label}) \cdot \frac{PLD}{e^{T1_b}}}{2 \cdot \alpha \cdot T1_b \cdot SI_{PD} \cdot (1 - e^{-\frac{\tau}{T1_b}})} \ [ml/100g/min]$$

This formula includes the control-label subtraction ($SI_{control} - SI_{label}$), and accounts for the labelling duration (τ), the PLD, the decay rate of the label defined by the longitudinal relaxation of blood in seconds ($T1_b$), and the labelling efficiency (α). Additionally, a separate image without background suppression called a proton-density-weighted image or a M0 image (SI_{PD}), is used to estimate the intensity of the signal that created the label. A brain/blood partition coefficient (λ) accounts for the difference between tissue and blood signal intensity. The factor of 6000 converts quantitative CBF values in the typical units of ml per 100 g per minute (ml/100g/min). The recommended values for labelling duration in PCASL is 1800 ms and 0.85 for labelling efficiency (Alsop et al., 2015). It is suggested CBF quantification is most sensitive to individual variability in $T1_b$, as this is directly affected by blood thickness (hematocrit (Hct)) (Lu, Clingman, Golay, & van Zijl, 2004), which has been shown to fluctuate in a diurnal manner (Sennels, Jørgensen, Hansen, Goetze, & Fahrenkrug, 2011). However, when this cannot be measured, the recommended standard value for $T1_b$ is 1650 ms (Alsop et al., 2015)

1.7 The present study

In spite of a large body of research, the fundamental function of sleep is not completely understood. Since synaptic strength increases during wake and decreases during sleep (as predicted by the synaptic homeostasis hypothesis), brain metabolism should also increase throughout the waking hours and decrease during sleep, since synaptic activity is responsible for most of the brain energy metabolism (Attwell & Laughlin, 2001). Indeed, brain

metabolism has been shown to increase from morning to afternoon and decrease after sleep (Bartlett et al., 1988; Boyle et al., 1994; Vyazovskiy et al., 2008). However, other studies have found the opposite effect, with decreases from morning to afternoon (Hodkinson et al., 2014) and no changes (Shannon et al., 2013). Importantly, to our knowledge, no studies have explored metabolism specifically in the thalamus throughout the day.

Differences in sleep chronotypes, which refers to an individual circadian rhythm type (Horne & Ostberg, 1976), has been associated with differences in circadian signalling and sleep pressure build-up. For example, evening types, which prefer to wake up later in the morning and go to sleep later at night than morning types, have a slower build-up of homeostatic sleep pressure than morning types (Taillard, Philip, Coste, Sagaspe, & Bioulac, 2003). Sustained attention in evening types compared to morning types has also been associated with higher SCN activity (Schmidt et al., 2009). Concerning the role of the thalamus in attention and the possible link to SCN, differences in sleep chronotypes might be a potential confound and need to be addressed.

Furthermore, it is important to assess the participants' prior sleep-wake cycle, which can be done with polysomnography (PSG), actigraphy or self-reported sleep diaries. PSG records numerous physiological parameters related to sleep and wake, such as electrical brain activity, eye movements, muscle activity, heart rate and respiratory function (Marino et al., 2013). Although PSG is a widely used and reliable technique, actigraphy is often used in sleep research due it being less expensive and being a more convenient and non-invasive method, which is why this method was employed in the current study. Actigraph devices, usually worn on the wrist, record body movements to assess sleep or wake states and has found to be a valid method to estimate daily sleep-wake cycles over an extended time in a person's natural environment (Martin & Hakim, 2011).

One could argue that prolonged wakefulness should be associated with an increase in CMR in relation to the synaptic homeostasis hypothesis (Feinberg & Campbell, 2010). However, no studies have reported increases in global CMR when wakefulness is extended by a night of total sleep deprivation, only decreases (Thomas et al., 2003) or regional increases specific to the visual cortex (Wu et al., 2006). However, it has been suggested that although prolonged wakefulness is associated with increased metabolic demand, the brain metabolism might not increase (Vyazovskiy, Tobler, Cirelli, & Tononi, 2009). The decreases in metabolic rate seen after sleep deprivation might reflect metabolic overload, which leads to synaptic failure. If

metabolism decreases in arousal-promoting areas, it could explain the observed arousal and attentional deficits seen after sleep deprivation. As CMR correlates well with CBF (Raichle, Grubb, Gado, Eichling, & Ter-Pogossian, 1976), ASL perfusion MRI can be used to investigate this hypothesis.

As the thalamus plays a key role in the arousal system and cortical attention network (Lim & Dinges, 2008) and sleep deprivation results in decreased arousal, impaired attention and other cognitive deficits (Lim & Dinges, 2010), this subcortical structure seems particularly sensitive to sleep deprivation. Indeed, several neuroimaging studies report reduction in thalamic activity after sleep deprivation, (Shao et al., 2013; Thomas et al., 2003; Wu et al., 2006). However, other studies how found increased thalamic activation after sleep deprivation (Tomasi et al., 2009). Thus, further investigation is needed to establish the effects of sleep deprivation on thalamic activity.

The acute antidepressant effect seen after sleep deprivation becomes evident after one night of sleep deprivation and greatest when patients are exposed to daytime light (Benedetti & Colombo, 2011). Thus, investigating sleep deprivation beyond 24 hours might shed some light on the neurobiological mechanisms occurring after 32 hours of sleep deprivation. We expected to see further CBF decreases, but as the thalamus also receives circadian information inputs, it might have some influence when sleep deprivation is prolonged to the second day.

As such, the current study aims to further explore diurnal variability and sleep deprivation variability in thalamic CBF after a day of normal wake and acute sleep deprivation using PCASL perfusion MRI. Based on the previous research, the following hypothesis are proposed:

1. A day of wake (12 hours of wake) will lead to increases in thalamic CBF.

2. 24 hours with sleep deprivation will lead to decreases in thalamic CBF.

3. 32 hours with sleep deprivation will lead to further decreases in thalamic CBF

2. METHODOLOGY

2.1 Ethics

The project was approved by the Regional Committees for Medical and Health Research Ethics (REK: 2017/2200) and registered in the Division of Radiology and Nuclear Medicine (KRN: 1730). The participants read and signed a consent form prior to participation and were informed about their right to withdraw from the experiment at any given time. This was done in accordance with the Helsinki Declaration.

2.2 Participants

Ten right-handed participants were recruited for the study (2 females). To be eligible for participation the participants had to be from 18 to 50 years of age. The exclusion criteria were any neurological or psychiatric disorders (including sleep disturbances), recent use of psychotropic drugs, cigarette smoking and standard MRI exclusion criteria such as metal or electronic implants (e.g., pacemaker, brain aneurysm clip) and claustrophobia. One participant had an arachnoid cyst but was not excluded as the cyst was located in the temporal lobe and this current study investigated changes specifically in the thalamus. Participants received NOK 1000 as compensation for their participation. Demographics and sleep measurements are summarized in Table 3.

2.3 Study protocol

The MRI sessions were conducted at the Oslo University Hospital (OUH) on four occasions (see Figure 4). The first two sessions were carried out in the morning after a night of regular sleep in their own beds (time point (TP) 1) and then in the evening approximately 12 hours later (TP2). Participants were scanned a third time (TP3) the next morning after being sleep deprived (24 hours awake), and the fourth and final MRI session (TP4) was conducted in the afternoon after approximately 32 hours of wake. Throughout the study, the participants stayed under constant supervision at the hospital. They followed a standardized activity plan (see Appendix 1), including light physical activity, being on their computer and playing board games. Light psychical activity included 30 minutes walks outside around the OUH area. Time in front of a computer screen was not allowed two hours prior to each MRI

session, as light-emitting electronic devices can affect the circadian rhythm and temporarily increase alertness (Chang, Aeschbach, Duffy, & Czeisler, 2015). Caffeine consumption was allowed according to their usual amount, but asked to abstain for six hours prior to each MRI session. Food and beverages were provided throughout the study and they were allowed to use nicotine (in form of "snus") according to their usual amount, but no intake of food or nicotine usage was allowed two hours prior to each MRI session. To control for food and fluid intake, recommended calorie-intake for each participant was estimated using a calculator provided by the Norwegian Health Informatics (Norsk Helseinformatikk, 2015). This standardized activity plan was employed in order to control for potential confounds, as it is established that numerous factors could influence brain perfusion (Clement et al., 2017).

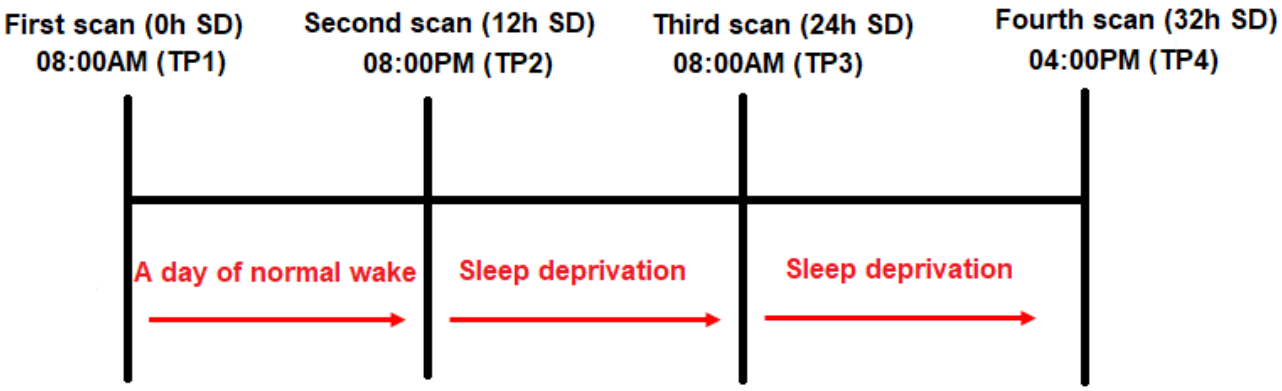

Figure 4. The participants underwent MRI sessions in the morning (TP1) after a night of sleep in their own beds, approximately 12 hours (h) later in the evening (TP2), the next morning (TP3) after being sleep deprivated for approximately 24 h, and then the following afternoon (TP4) after 32 h of sleep deprivation.

2.4 Materials

2.4.1 Assessment of individual sleep patterns

Prior to the first MRI session, all participants were instructed to fill out a sleep diary (Bjorvatn, 2010) and wear an actigraph on their wrist for 5-7 consecutive days in advance to assess their sleeping patterns.

The sleep diary (Bjorvatn, 2018) included questions about their sleep and wake times and sleep quality (see appendix 2), and was modified in the current study to include caffeine and

nicotine usage. The participants were asked to fill out this 12-item scale daily. Additionally, to objectively measure their sleep cycle, the participants wore an actigraph- a motion sensor-, which measures physical movement and light (MotionWatch8, CamNtech, Cambridge, UK,). Data were sampled in 1-minute epochs and analysed using the MotionWare Software, version 1.2.5.

2.4.2 Sleep-related questionnaires

The participants completed five questionnaires probing chronotype and sleep quality. Epworth Sleepiness Scale (ESS), an eight-item self-rating scale, was used to measure the degree of daytime sleepiness with higher scores indicating higher daytime sleepiness levels, with scores over 10 suggest significant daytime sleepiness (Johns, 1991). Pittsburgh Sleep Quality Index (PSQI), containing 19 self-administrated questions assessed their sleep quality during the past month (Buysse, Reynolds, Monk, Berman, & Kupfer, 1989). Better sleep quality is associated with lower scores, with scores > 5 indicating significant disturbed sleep quality. To assess individual chronotype, the Morningness-Eveningness Questionnaire (MEQ) was used, containing 19 questions targeting the participants' preferences for wake and sleep times (Horne & Ostberg, 1976). The scores indicate the degree to which a person is a morning type (higher scores) or an evening type (lower scores). Global Sleep Assessment Questionnaire (GSAQ), including 11 items, was used to detect potential sleep disturbances and sleep disorders (Roth et al., 2002). Higher scores indicate higher levels of sleep-related problems. Bergen Insomnia Scale, a six-item scale, was used to address insomnia symptoms during the past month (Pallesen et al., 2008), with higher scores indicating a higher prevalence of symptoms.

2.4.3 Acute sleepiness measurements

To measure acute sleepiness and alertness throughout the study, subjective and objective measures were used every second hour. Karolinska Sleepiness Scale (KSS), a 9-point scale (Åkerstedt & Gillberg, 1990), and Stanford Sleepiness Scale (SSS), a 7-point scale (Hoddes, Zarcone, Smythe, Phillips, & Dement, 1973), were the subjective measures addressing the degree of sleepiness. KSS ranges from 1 ("extremely alert") to 9 ("extremely sleepy") and SSS ranges from 1 ("feeling active or wide awake") to 7 ("no longer fighter sleep, sleep onset soon"). In addition, a personal computer (PC)-based psychomotor vigilance test (PC-PVT),

version 1.1.0, was used to objectively measure participants' sustained attention (Khitrov et al., 2014). This is a 5-minute task in which participants were instructed to respond as quickly as possible to visual stimuli appearing on a computer screen at random inter-stimulus intervals ranging from 2 to 10 seconds. All participants did a practice run before the first PC-PVT test. For the current study, median and variance (the difference between the maximum and minimum) in reaction time was used for the analysis. The task was run with Matlab R2017a (MathWorks Inc., Natick, MA, USA) and performed on a 15.6-inch Lenovo V510-15IKB laptop (Windows 10 Pro) at a display resolution of 1920 x 1800 and a refresh rate of 60 Hz. A Dell N889 USB Optical mouse- MS111-P was used with a movement resolution of 1000 dots per inch.

2.4.4 MRI acquisition

MRI data was acquired from a 3T Siemens Prisma scanner, equipped with a 32-channel head coil at Oslo University Hospital. CBF was measured and quantified using a PCASL sequence with a single-shot 3D gradient and spin echo (GRASE) image readout (matrix = 63 x 64, FoV = 256 x 256 mm^2, 42 axial slices, slice thickness = 3.4 mm, TE/TR = 17.56/4430 ms and FA = 180°). The labelling duration was set to 1800 ms and the PLD to 1800 ms (FA = 28°), as recommended (Alsop et al., 2015). To visualize precerebral vessels before planning the ASL scan, a 2D time-of-flight (TOF) angiogram was acquired with 30 transverse slices (voxel size = 0.5 x 0.5 x 2.5 mm) and with following parameters: TE/TR = 4.65/20 ms, FoV = 256 x 256 mm^2, FA= 60° and acquisition matrix = 256 x 256. Based on the individual TOF angiogram, the labelling plane was placed perpendicular to the vertebral arteries and the internal carotid arteries (Figure 5). To improve SNR, background suppression was achieved by using two saturation pulses during the PLD to remove much of the static tissue signal within the imaging region (Alsop et al., 2015). Fifteen control-label pairs were obtained. In addition, a proton-density-weighted reference image (M0) with identical acquisition parameters as the PCASL scan, but without background suppression. Structural images were acquired using T1-weighted multi-echo magnetization-prepared rapid gradient echo imaging (MEMP-RAGE) of 176 sagittal slices with voxel sizes of 1 x 1 x 1 mm with the following parameters: echo time (TE) = 1.69, 3.55, 5.41 and 7.27 ms, repetition time (TR) = 2530 ms, T1 = 1100 ms, flip angle (FA) = 7°, field of view (FoV) = 256 x 256 mm^2, matrix = 256 x 256. These images were used for registration and segmentation of the thalamus. Participants were instructed to refrain from moving and keep their eyes open during scanning. Scan

duration was approximately 14 minutes in total for the sequences described above. See Appendix 3 for the MRI scan protocol. Two participants were scanned twice during the third session since they nearly fell asleep, and scans were aborted to give them a chance to stretch their legs in order to finalize scans without falling asleep.

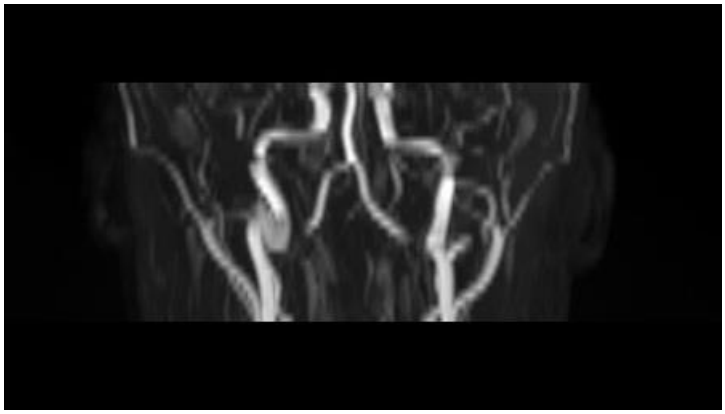

Figure 5. A representative TOF-angiogram of one participant.

2.5 MRI analysis

2.5.1 Post-processing

ASL-analysis

The ASL-analysis was performed using nordicICE (nICE; NordicNeuroLab, Bergen, Norway). Motion correction was applied to the separate control and label images, pairwise subtraction was performed and outliers were excluded. Quantification of CBF was achieved by including the following parameters: $T1_b$ = 1650 ms, which is the standard value for 3T MRI and labelling efficiency = 0.85 (Alsop et al., 2015). Additionally, pixel-wise calibration was applied using the M0 reference image, with a scanning specific scaling factor of 15 for the M0 images.

Thalamus masks

For each participant, the four T1-weighted structural images were co-registered and averaged together using FreeSurfer (FreeSurfer Software Suite, https://surfer.nmr.mgh.harvard.edu/), version 6.0) for increased SNR and segmentability. The

pipeline in FreeSurfer included a skull strip, as well as an automatic subcortical segmentation, using a probabilistic atlas (Fischl et al., 2002), of each participant's averaged structural image. All CBF maps for each participant were then co-registered to their averaged structural image in nICE, following an extraction of subject-specific thalamus masks from the subcortical segmentation.

2.5.2 Region-of-interest (ROI) analysis

ROI analysis was performed in nICE. The thalamus segmentation from FreeSurfer was used to extract subject-specific CBF-values from the thalamus (Figure 6). The statistical analysis was performed using Statistical Package for the Social Sciences (SPSS), version 25 for Windows (IBM Corp, Armonk, NY), and given the design of the study was a within-subject design, repeated-measures analysis of variance (ANOVA) was used to analyse the ASL data and acute sleepiness measures. Pairwise comparisons of the estimated marginal means were conducted as a *post hoc* test, and correction of multiple comparisons was achieved by applying a Bonferroni correction. Pearson's correlation analysis was conducted to investigate the relationship between thalamic CBF-values and chronotype (MEQ), subjective sleepiness measures (SSS and KSS) and objective sleepiness measures (PC-PVT).

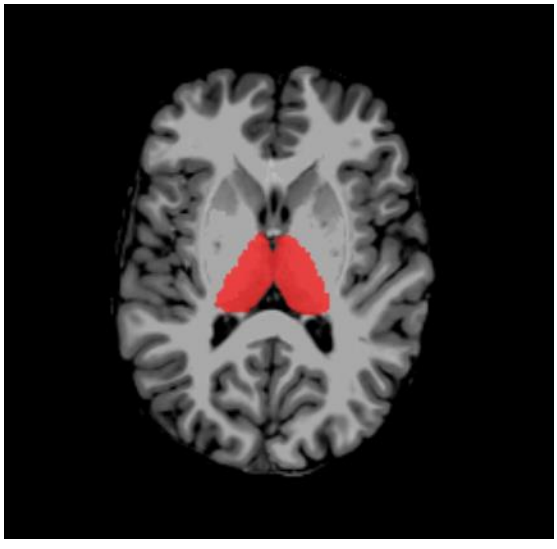

Figure 6. CBF-map of a representative participant at TP1.

3. RESULTS

CBF-maps of all participants at each time point is presented in Figure 7. Although not excluded, some CBF-maps appear to be of lower quality, which might be due to labelling failure (participant 7 and 8; Figure 7B).

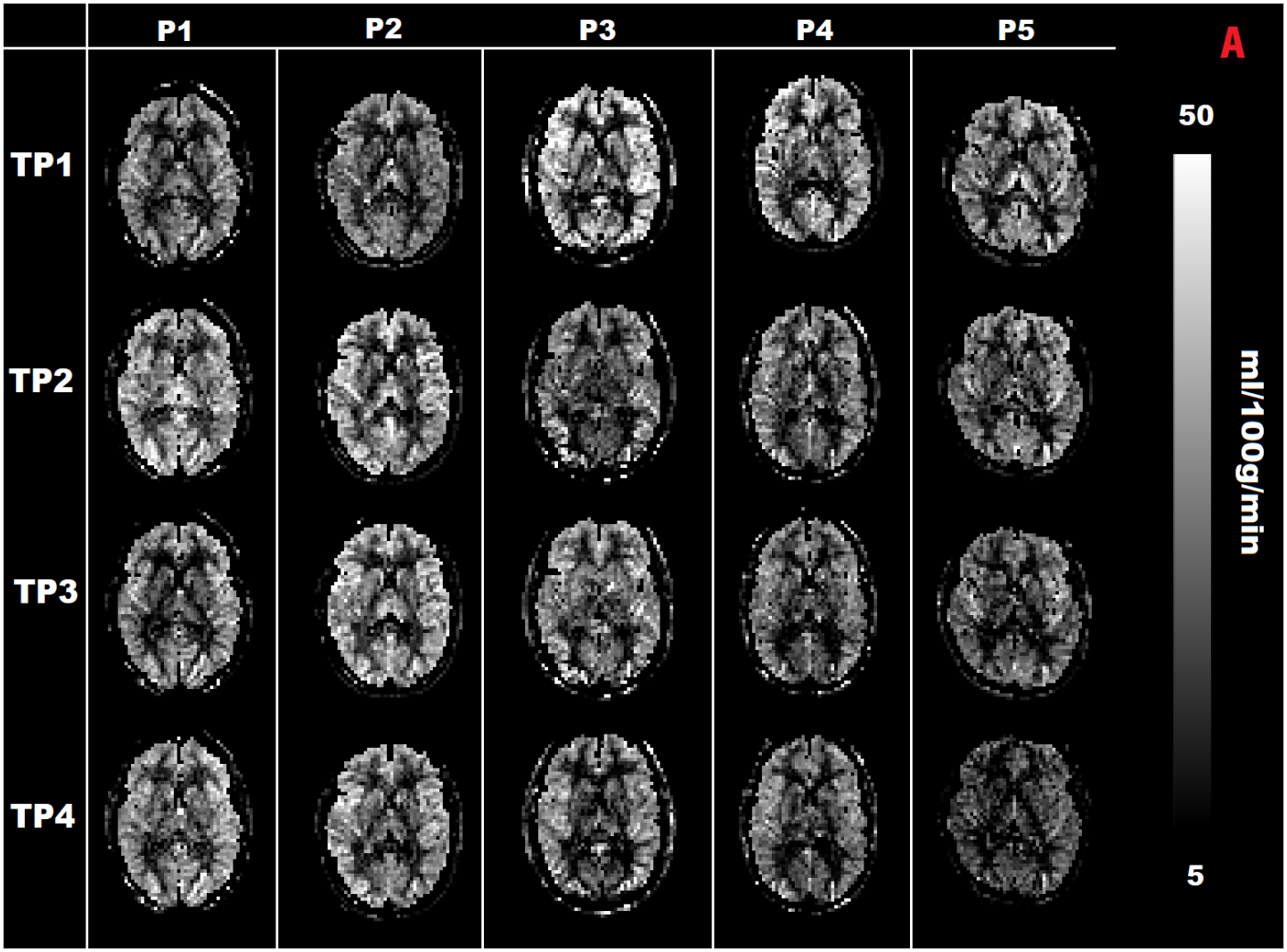

Figure 7a. CBF-maps of participants (P)1 to 5 at each time point (TP). Scale shows the CBF in mL/100g/min.

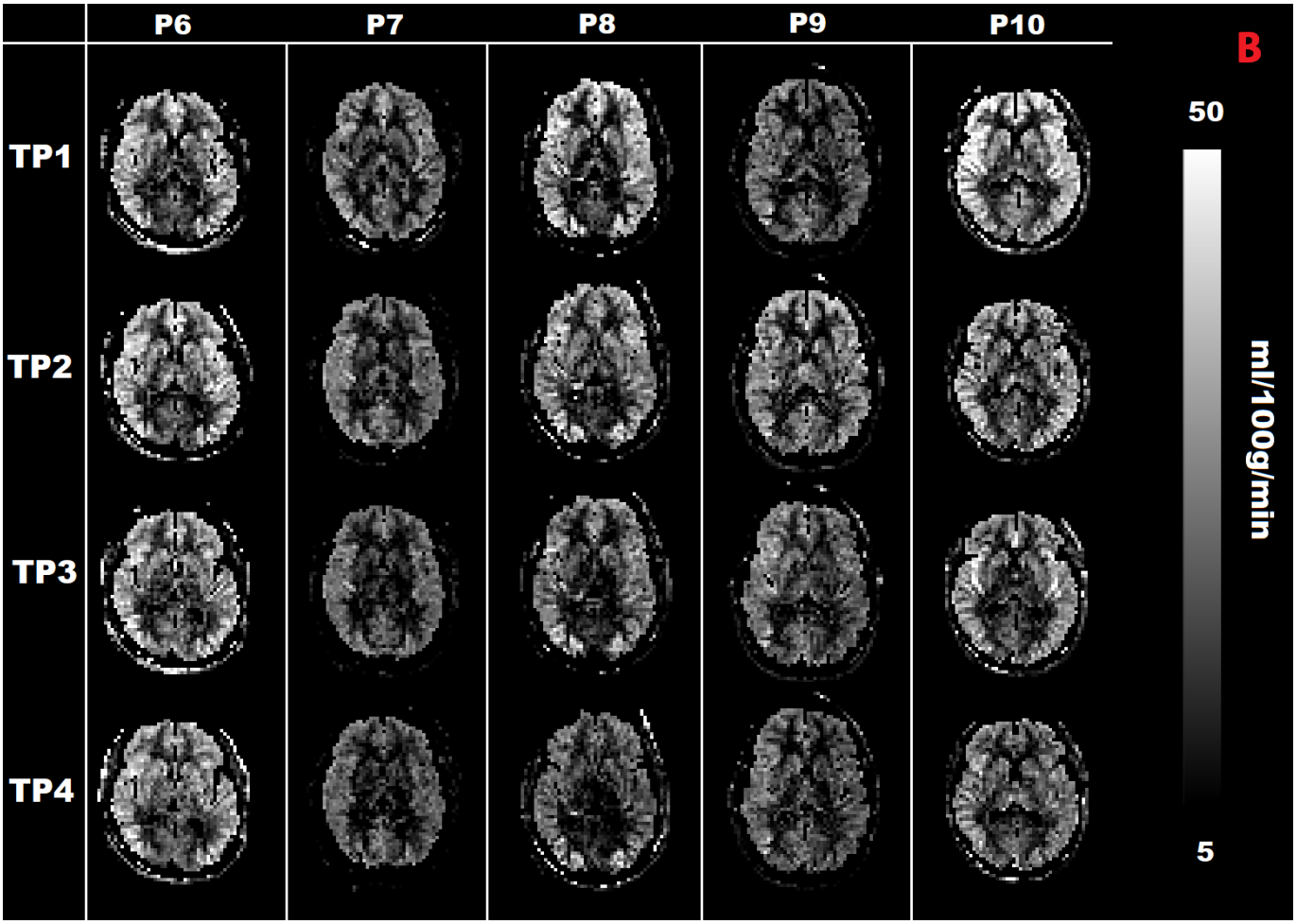

Figure 7B. CBF-maps of participants (P) 6 to 10 at each time point (TP). Scale shows the CBF in mL/100g/min.

3.1 Thalamic CBF changes

Figure 8 shows the individual thalamic CBF-changes across the different time points. The repeated measures ANOVA showed that there was a significant main effect of waking hours on thalamic CBF, $F(3, 27) = 5.12$, $p < 0.05$. Pairwise comparisons of the estimated marginal means were conducted to further investigate any differences between the time points.

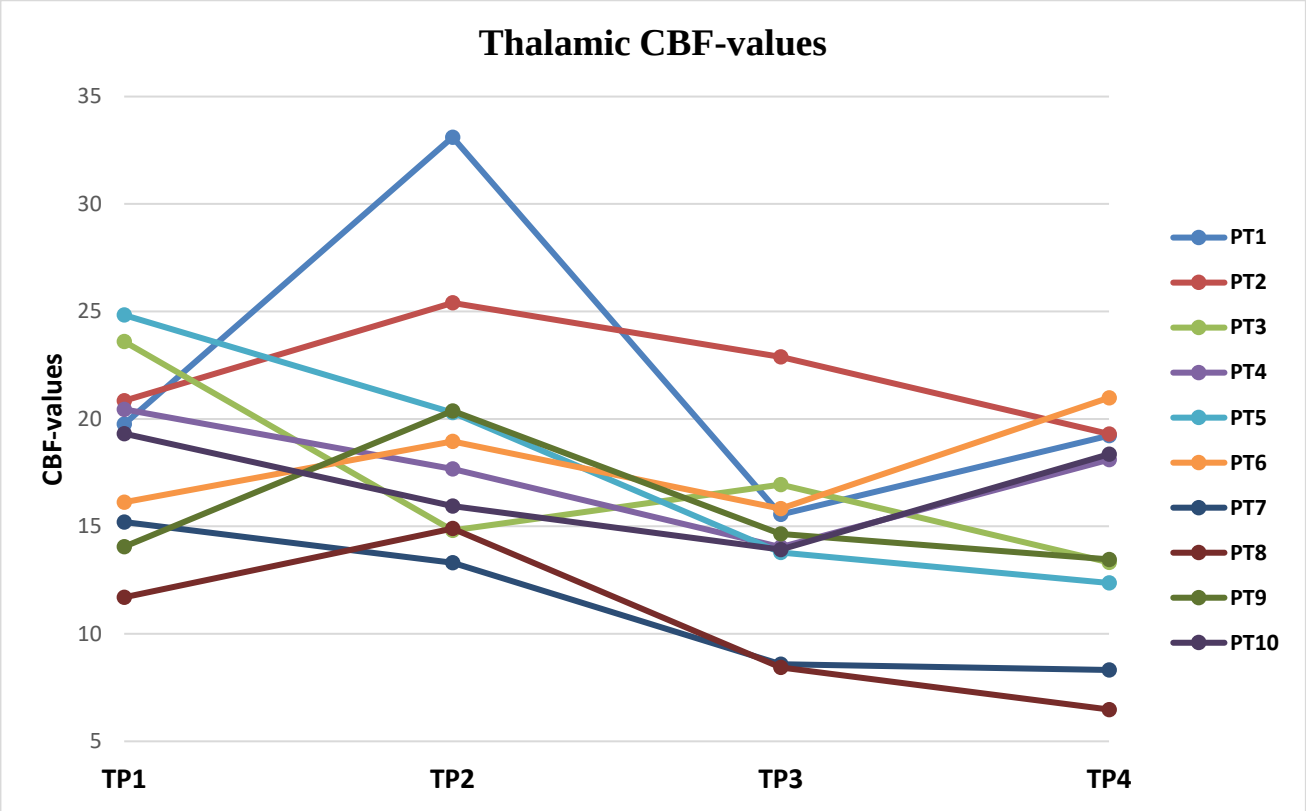

Figure 8. Individual plots of thalamic CBF-values at the different time points

A day of normal wake (TP1 to TP2)

There was a 4.9 % mean increase in thalamic CBF from TP1 (M = 18.59, SD = 4.22) to TP2 (M = 19.48, SD = 5.95). However, the pairwise comparison, with Bonferroni-adjusted p-values, showed no significant difference between the time points ($p > 0.999$).

A night of sleep deprivation (TP2 to TP3)

Although there was a large mean decrease (25.7 %) in thalamic CBF from TP2 (M = 19.48, SD = 5.95) to TP3 (M =14.46, SD = 4.1), this did not reach significance with the multiple comparison correction, p = 0.075.

24 hours of sleep deprivation (TP1 to TP3)

There was a 22.2 % mean decrease in thalamic CBF from TP1 (*M* = 18.59, *SD* = 4.22) to TP3 (*M* =14.46, *SD* = 4.1), however this did not survive multiple comparisons correction, *p* = 0.058.

32 hours of sleep deprivation (TP1 to TP4)

32 hours of sleep deprivation, from TP1 *(M* = 18.59, *SD* = 4.22) to TP4 (*M* = 14.99, *SD* = 4.97) showed a 19.3 % mean decrease, however this was not significant with the multiple comparison correction, *p* = 0.33. Comparisons between TP3 to TP4 showed that there was a 3.7 % mean increase in thalamic CBF, however this was also not significant (*p* > 0.999).

3.2 Measures of chronotype and acute sleepiness

Mean values and SD for the subjective sleepiness measures (KSS and SSS) and PC-PVT median and variance are summarized in Table 1 and chronotype in Table 2. Repeated measures ANOVA revealed that there was a significant main effect on waking hours on both subjective sleepiness measurements; KSS, F(3, 27) = 15.2, p < 0.001 and SSS, F(3, 27) = 17.86, *p* <0.001. Bonferroni corrected pairwise comparisons showed that the participants were significantly more tired at TP3 and TP4 when compared with TP1, both *p* < 0.05. There was also a significant difference between TP2 and TP3, *p* < 0.05. There was no significant difference in sleepiness between TP3 and the TP4 or between TP1 and TP2 (both *p* > .999). There was no significant difference in the PC-PVT measurements (MedianRT and VarianceRT) between the different time points (*p* > 0.05).

Table 1. *Mean and standard deviation (SD) for sleepiness scales (KSS and SSS), sleep chronotype (MEQ) and PC-PVT median and variance in reaction time for each time point.*

	TP1	**TP2**	**TP3**	**TP4**
KSS	3.2 *(1.99)*	3.8 *(2.62)*	7.2*(1.93)*	7.1 *(1.29)*
SSS	2.3*(1.25)*	2.7*(1.42)*	5.9 *(1.2)*	4.7 *(1.25)*
MedianRT	236.60 *(34.11)*	243.69 *(36.10)*	273.25 *(53.37)*	263.61 *(34.47)*
VarianceRT	413.56 *(145.12)*	234.33 *(29.98)*	2376.22 *(2046.95)*	359.56 *(81.08)*

Mean and SD for sleepiness scales and median and variance in reaction time (RT) for each time point (TP), reported in milliseconds.

Table 2. *Correlations between sleepiness measurements and chronotype and CBF-values at the different time points (TP).*

	KSS		**SSS**		**PC-PVT medianRT**		**PC-PCV varianceRT**		**MEQ**	
	R	***P***	***R***	***P***	***R***	***P***	***R***	***P***	***R***	***P***
TP1	.23	.53	.13	.72	.32	.4	.31	.42	.4	.25
TP2	.69*	.03	.58	.08	.7*	.01	.41	.24	-.01	.98
TP3	.39	.27	.58	.08	.11	.77	-.5	.14	.05	.9
TP4	-.16	.65	-.15	.68	.54	. 11	.07	.84	.16	.65

R = Pearson's correlation coefficient, P = p-value, * = significant at a .05 level

As shown in Table 2, there were no significant correlations between CBF-values at the different time points and subjective sleepiness (KSS and SSS), except for a positive correlation between CBF-values at TP2 and KSS (r = .69, p <0.05). Similarly, a positive correlation between CBF-values at TP2 and PC-PVT medianRT was found (r = .7, p < 0.05). There was no correlation between chronotype (MEQ) and CBF-values at neither time points.

3.3 Demographics and sleep-related measurements

Demographics and sleep-related measures are summarized in Table 3. All participants had normal sleep-wake cycles as reported in the sleep diaries and recorded by the actigraph. However, on average, the participants reported significantly less sleep the night before compared to the reported sleep duration the last week and month prior to the experiment (both p <0.01). The participants did not report significant daytime sleepiness (ESS < 10) or disturbance in sleep quality (PSQI scores < 5) in the last month.

Table 3. *Demographics and sleep-related characteristics*

Characteristic	**All subjects (*N* =10)**
Age (years), mean (SD)	26.30 *(4.97)*
Handedness (right)	100%
Gender (female/male)	2/8
PSQI, mean (SD)	4.40 (*2.41*)
MEQ, mean (SD)	46.30 (*9.44*)
Bergen Jnsomnia Scale, mean (SD)	7.80 (*3.62*)
ESS, mean (SD)	5.80 (*3.68*)
GSAQ, mean (SD)	21.30 (*3.20*)
Sleep per night (hours) the month prior to the study	7h34min ± 37min
Sleep per night (hours) the week prior to the study (sleep diary)	7h31min ± 46min
Hours of sleep before TP1 (sleep diary)	5h53min ± 1h17min
Sleep per night (hours) the week prior to the study (actigraphy)	7h49min ± 46min
Hours of sleep before TP1 (actigraphy)	6h10min ± 42min
MRI scanning time point (TP1)	08:27±36 min
MRI scanning time point (TP2)	19:47 ±22min
MRI scanning time point (TP3)	07:56 ±30 min
MRI scanning time point (TP4)	16:23 ± 24 min

Mean and standard deviations (±SD) for sleep-related questionnaires including the Pittsburg Sleep Quality Index (PSQI), Morningness-eveningness questionnaire (MEQ), Bergen Insomnia scale, Epworth Sleepiness Scale (ESS), Global Sleep Assessment Questionnaire (GSAQ), and hours of sleep and mean and SD of the scanning times of the MRI sessions (Time point (TP)).

4. DISCUSSION

The purpose of the study was to investigate thalamic CBF variability from morning to evening and after 24 and 32 hours of sleep deprivation. Specifically, it was hypothesised that thalamic CBF would increase from morning to evening (TP1 vs TP2), and decrease after 24 hours of sleep deprivation (TP1 vs TP3) and decrease after 32 hours of sleep deprivation (TP1 vs TP4). The results showed a significant main effect for time spent awake on thalamic CBF variability. However, when examined further, there was no significant difference between either of the time points. The most likely explanation for the lack of significant findings in thalamic CBF changes between each time point is the small sample size (N = 10). Although it is important to control for multiple comparisons to control for type I errors (false positives), the Bonferroni correction might have been too conservative given our small sample size involving multiple comparisons, and increased the likelihood of making a type II error (false negative) (Field, 2013), thus yielding non-significant results when differences might actually exist.

4.1 Thalamic CBF changes from morning to evening

It was hypothesised that thalamic CBF would increase from morning (TP1) to evening (TP2). Although there was a 4.9 % mean increase in thalamic CBF, this did not reach significance. In relation to the synaptic homeostasis hypothesis, in which wakefulness is associated with increases in synaptic strength, and in turn increases in metabolism, we expected to find increases in CBF as this correlates well with CMR (Raichle et al., 1976). As mentioned, the lack of significant result might be due to our small size. The research on diurnal variability in CBF and CMR is limited. One PET study showed a trend towards an increase in brain metabolism from morning to afternoon (Bartlett et al., 1988), and another PET study showed increased metabolism in hypothalamic and brainstem structures (Buysse et al., 2004). However, no changes in CMR and CBF has also been reported (Shannon et al., 2013). In an ASL study, no brain regions were associated with increases in blood flow, only found decreases in regions associated with the default network (Hodkinson, et al., 2014). The conflicting results, including the previous research and the current study, could be due to variation in sample sizes, the study design and neuroimaging methods. Furthermore, it is important to mention that these studies did not investigate changes specifically in the

thalamus. Thus, further research with larger sample sizes is needed to investigate thalamic CBF variation from morning to evening.

Moreover, it has been suggested that the circadian signal is strongest in the evening to prevent us from falling asleep (Gaggioni et al., 2014). As it has been proposed that the PVT in the intralaminar/midline thalamic nuclei receives circadian information from the SCN (Colavito et al., 2015), one might expect higher thalamic activity and in turn increased thalamic CBF in the evening. Differences in sleep chronotypes have been associated with differences in SCN activity, in which sustained attention in evening types compared to morning types has been associated with higher SCN activity (Schmidt et al., 2009). In the current study, there was a tendency towards participants being more moderately evening types than morning types. However, they were neither extreme morning or evening types and no correlations was found between sleep chronotypes and CBF-values. Thus, it is unlikely that this would have a large influence on the results.

Surprisingly, there was a positive correlation between KSS and CBF-values at TP2, indicating an association between more sleepiness and higher thalamic CBF in the evening. Similarly, a positive correlation between PC-PVT median RT and CBF-values at TP2 was found. However, this has to be interpreted with caution, as we did not correct for multiple comparisons. Previous research has shown that resting CBF activity, measured by PCASL, can predict subsequent PVT performance, with greater performance associated with higher resting CBF in the thalamus (Lim et al., 2010). The inconsistency might be due to differences task duration as the study by Lim et al. (2010) used a 20-minute task, whereas the current study employed a 5-minute task.

4.2 Thalamic CBF changes after 24 hours of sleep deprivation

It was hypothesised that 24 hours of sleep deprivation (TP1 vs TP3) would be associated with decreases in thalamic CBF. We also examined thalamic changes after one night of sleep deprivation (TP2 vs TP3). Although we found large mean decreases both after 24 hours of sleep deprivation (22.2 %) and one night of sleep deprivation (25.7%), none of these changes was significant after the multiple comparison correction.

As sleep deprivation results in decreased arousal and decreased cognitive performance, it was expected to found decreases in thalamic CBF after sleep deprivation. The thalamus is part

of the arousal-promoting system, where it is activated by wake-promoting cell groups in the brainstem, and the thalamus is crucial for transmitting information to the cortex where information is further processed (Saper, Scammell, et al., 2005). It is suggested that sleep deprivation might lead inhibition of cholinergic neurons in the brainstem, which in turn would alter the thalamic activity (Strecker et al., 2000) and thus influence cognitive performance. As mentioned, the lack of significant results might be due to the low sample size.

However, the thalamus is not a unitary structure but comprises several subnuclei with different functions and distinct anatomical connections (Sherman, 2007). The current study was not designed to investigate different thalamic subnuclei, thus the lack of significant findings might be a result of variability within individual thalamic nuclei. Specifically, the intralaminar/midline thalamic nuclei are suggested to mediate arousal to promote awareness (Van der Werf et al., 2002). Orexin neurons modulate activity in the intralaminar/midline thalamic nuclei (Govindaiah & Cox, 2006) and the effect of orexin decreases during sleep deprivation (Grivel et al., 2005). Indeed, Thomas et al. (2003) reported that the thalamic reductions following sleep deprivation were greatest in the midline thalamic nuclei. Thus, this suggests that these thalamic subnuclei might be particularly sensitive to sleep deprivation.

One study, using the same neuroimaging method as the current study, did not find changes in thalamic CBF after sleep restriction, only decreases in the frontoparietal cortex in the most drowsy participants (Poudel et al., 2012). However, this study did not look for changes after total sleep deprivation but used a less severe protocol in which participants were restricted to 4 hours of sleep. In addition, they observed great inter-individual behavioural differences. Thus, their results are difficult to compare to ours due to large differences in study design. Using a similar design as the current study, Thomas et al. (2000) found CMRglu decreases in thalamus after 24 hours of sleep deprivation using PET. Although the neuroimaging method was different than ours, CMR is known to correlates well with CBF (Raichle et al., 1976), thus similar changes were expected to be found in this current study. The inconsistent findings might again be due to sample size, as they had a larger sample size.

Although the participants in our study reported being more tired after 24 and 32 hours of sleep deprivation, correlations between CBF-values at TP3 and TP4 and subjective sleepiness (KSS and SSS) was not found. This is somewhat surprising, as the thalamus is involved in the arousal system and therefore lower thalamic CBF would be expected to associate with higher

sleepiness levels. However, the lack of significant correlations might be due to the small sample size.

4.3 Thalamic CBF changes after 32 hours of sleep deprivation

Although there was a 19.3 % mean decrease in thalamic CBF after 32 hours of sleep deprivation (TP1 to TP4), this was not significant. Visual inspection of the individual thalamic CBF plots show a trend towards an increase from TP3 to TP4, with a non-significant 3.7 % mean increase. Although speculative, circadian signalling might somewhat counteract the increased sleep pressure when sleep deprivation exceeds the 24-hour circadian cycle. Thus, the non-significant finding from TP1 to TP4 might be due to influences from circadian rhythms promoting arousal and alertness when sleep deprivation is prolonged into a second circadian cycle. However, when sleep deprivation is even further prolonged, sleep pressure might override circadian processes again. Indeed, Thomas et al. (2003) found even further decreases in the thalamus from 24 hours to 48 and 72 hours of sleep deprivation.

4.4 Limitations and future directions

As previously discussed, the largest limitation of the current study was the sample size. Thus, the lack of significant findings are likely influenced by insufficient power, as the study only recruited ten participants due to time constraints. Furthermore, from visual inspection, it appeared that two of the PCASL scans suffered from low quality, and this might be due to labelling failure and thus affecting the CBF-values. Although the participants had lower CBF-values compared to the other participants, this was consistent through all four scans. However, as it might have affected the results on a group level, and should perhaps have been excluded from further analysis.

The participants reported on average a normal amount of sleep in the month and week prior the experiment that is recommended for healthy individuals (Watson et al., 2015). However, they reported less sleep the night before the experiment, which might have affected their baseline sleep homeostasis and in turn influenced thalamic CBF changes.

CBF can be influenced by several physiological factors (Clement et al., 2017). Although, the current study controlled for various potential confounds such as caffeine, nicotine, physical activity, sleep quality and sleep habits, there will always be other factors affecting

our CBF estimations. For example, the study did not control variability in $T1_b$. Since $T1_b$ values determine the decay rate of spin-labelled blood water (Alsop et al., 2015), it affects the quantification of CBF. The analysis in the current study used a constant value for $T1_b$ (1650 ms). However, blood thickness (Hct), which directly affects $T1_b$ (Lu et al., 2004), is known to fluctuate in a diurnal manner (Sennels et al., 2011), and in turn, reduced the accuracy of our CBF estimations. Thus, future studies should take blood samples to measure Hct levels and use Hct-corrected $T1_b$ values in the quantification of CBF. Furthermore, we included both females and males in our sample. It has been reported that CBF is higher in females than in males (Clement et al., 2017), however, a study by Henriksen et al. (2013) suggests that the gender-related CBF differences are mostly explained by lower Hct-levels in females.

Furthermore, a standard computer mouse was used in the PC-PVT, whereas gaming mice with higher movement resolution show a significant advantage in response detection (Khitrov et al., 2014), thus it might have led to some inaccuracy when measuring reaction times. However, as the same computer mouse was used throughout the experiment for every participant, it is unlikely that this would have a substantial effect on the results.

As mentioned, we did not investigate changes within the different thalamic nuclei, which might have affected the results. Although it is difficult to segment the thalamus from T1-weighted images due to its diffuse contrasted boundaries (Zhang, Lu, Feng, & Zhang, 2017), future studies should use a similar approach as the current study, in which we were able to acquire several T1-images of each participant and in turn improving the SNR and achieve a great thalamic segmentation.

In relation to the antidepressant effect of sleep deprivation, future studies should investigate CBF changes after sleep deprivation in patients with depressive disorder. As it is suggested that depression is associated with impaired synaptic plasticity (Wolf et al., 2016), the antidepressant effect might be due to the synaptic abnormalities being repaired by an increased synaptic strength associated with wake, as predicted by the synaptic homeostasis hypothesis. Depression is also associated with disturbed circadian rhythms (McClung, 2007), and as the PVT receives projections from the SCN and is also connected to mood-regulating structures (Hsu et al., 2014), this nuclei might be a link between abnormalities in circadian rhythms and depression.

4.4 Conclusion

The current study investigated thalamic CBF variability from morning to evening and after sleep deprivation. Although we observed a 4.9 % increase from morning to evening, 22.2 % decrease after 24 hours and 19.3 % decrease after 32 hours of sleep deprivation, it did not reach significance. The lack of significant results is likely explained by our small sample size accompanied by a conservative multiple comparison correction. Furthermore, as we did not control for variability in $T1_b$, this reduced the accuracy in our CBF quantification. Further investigation is needed to explore these interesting trends towards changes in thalamic CBF from morning to evening and after sleep deprivation.

5. REFERENCES

Åkerstedt, T., & Gillberg, M. (1990). Subjective and Objective Sleepiness in the Active Individual. *International Journal of Neuroscience*, *52*(1–2), 29–37. https://doi.org/10.3109/00207459008994241

Åkerstedt, T., Philip, P., Capelli, A., & Kecklund, G. (2011). Sleep loss and accidents-Work hours, life style, and sleep pathology. *Progress in Brain Research*, *190*, 169–188. https://doi.org/10.1016/B978-0-444-53817-8.00011-6

Alam, M. A., Kumar, S., McGinty, D., Alam, M. N., & Szymusiak, R. (2014). Neuronal activity in the preoptic hypothalamus during sleep deprivation and recovery sleep. *Journal of Neurophysiology*, *111*(2), 287–299. https://doi.org/10.1152/jn.00504.2013

Alsop, D. C., Detre, J. A., Golay, X., Günther, M., Hendrikse, J., Hernandez-Garcia, L., … Zaharchuk, G. (2015). Recommended implementation of arterial spin-labeled perfusion MRI for clinical applications: A consensus of the ISMRM perfusion study group and the European consortium for ASL in dementia. *Magnetic Resonance in Medicine*, *73*(1), 102–116. https://doi.org/10.1002/mrm.25197

Attwell, D., & Laughlin, S. B. (2001). An Energy Budget for Signaling in the Grey Matter of the Brain. *Journal of Cerebral Blood Flow & Metabolism*, *21*(10), 1133–1145. https://doi.org/10.1097/00004647-200110000-00001

Bartlett, E. J., Brodie, J. D., Wolf, A. P., Christman, D. R., Laska, E., & Meissner, M. (1988). Reproducibility of cerebral glucose metabolic measurements in resting human subjects. *Journal of Cerebral Blood Flow and Metabolism*, *8*(4), 502–512. https://doi.org/10.1038/jcbfm.1988.91

Benedetti, F., & Colombo, C. (2011). Sleep Deprivation in Mood Disorders. *Neuropsychobiology*, *64*, 141–151. https://doi.org/10.1159/000328947

Bjorvatn, B. (2018). Søvndagbok. Retrieved from https://helse-bergen.no/nasjonal-kompetansetjeneste-for-sovnsykdommer-sovno/sovndagbok-sovno

Boyle, P. J., Scott, J. C., Krentz, A. J., Nagy, R. J., Comstock, E., & Hoffman, C. (1994). Diminished brain glucose metabolism is a significant determinant for falling rates of systemic glucose utilization during sleep in normal humans. *The Journal of Clinical Investigation*, *93*(2), 529–35. https://doi.org/10.1172/JCI117003

Bushey, D., Tononi, G., & Cirelli, C. (2011). Sleep and synaptic homeostasis: Structural evidence in Drosophila. *Science*, *332*(6037), 1576–1581. https://doi.org/10.1126/science.1202839

Buxton, O. M., Cain, S. W., O'Connor, S. P., Porter, J. H., Duffy, J. F., Wang, W., … Shea, S. A. (2012). Adverse metabolic consequences in humans of prolonged sleep restriction combined with circadian disruption. *Science Translational Medicine*, *4*(129), 129ra43. https://doi.org/10.1126/scitranslmed.3003200

Buxton, R. B., Frank, L. R., Wong, E. C., Siewert, B., Warach, S., & Edelman, R. R. (1998). A general kinetic model for quantitative perfusion imaging with arterial spin labeling. *Magnetic Resonance in Medicine*, *40*(3), 383–396. https://doi.org/10.1002/mrm.1910400308

Buysse, D. J., Nofzinger, E. A., Germain, A., Meltzer, C. C., Wood, A., Ombao, H., … Moore, R. Y. (2004). Regional brain glucose metabolism during morning and evening wakefulness in humans: preliminary findings. *Sleep*, *27*(7), 1245–54. https//doi:10.1093/sleep/27.7.1245

Buysse, D. J., Reynolds, C. F., Monk, T. H., Berman, S. R., & Kupfer, D. J. (1989). The Pittsburgh sleep quality index: A new instrument for psychiatric practice and research. *Psychiatry Research*, *28*(2), 193–213. https://doi.org/10.1016/0165-1781(89)90047-4

Chang, A.-M., Aeschbach, D., Duffy, J. F., & Czeisler, C. A. (2015). Evening use of light-emitting eReaders negatively affects sleep, circadian timing, and next-morning alertness. *Proceedings of the National Academy of Sciences of the United States of America*, *112*(4), 1232–7. https://doi.org/10.1073/pnas.1418490112

Chappell, M., MacIntosh, B., & Okell, T. (2017). *Introduction to perfusion qualification using arterial spin labeling* (First). Oxford University Press. https//doi:10.1093/oso/9780198793816.001.0001

Clement, P., Mutsaerts, H. J., Václavů, L., Ghariq, E., Pizzini, F. B., Smits, M., … Achten, E. (2017, April 10). Variability of physiological brain perfusion in healthy subjects – A systematic review of modifiers. Considerations for multi-center ASL studies. *Journal of Cerebral Blood Flow and Metabolism*, p. 0271678X1770215. https://doi.org/10.1177/0271678X17702156

Colavito, V., Tesoriero, C., Wirtu, A. T., Grassi-Zucconi, G., & Bentivoglio, M. (2015). Limbic thalamus and state-dependent behavior: The paraventricular nucleus of the thalamic midline as a node in circadian timing and sleep/wake-regulatory networks. *Neuroscience & Biobehavioral Reviews*, *54*, 3–17. https://doi.org/10.1016/j.neubiorev.2014.11.021

Daan, S., Beersma, D. G., & Borbely, A. A. (1984). Timing of human sleep: recovery process gated by a circadian pacemaker. *American Journal of Physiology - Regulatory, Integrative and Comparative Physiology*, *246*(2). R161–R183. https://doi:10.1152/ajpregu.1984.246.2.r161

Fama, R., & Sullivan, E. V. (2015). Thalamic structures and associated cognitive functions: Relations with age and aging. *Neuroscience & Biobehavioral Reviews*, *54*, 29–37. https://doi.org/10.1016/J.NEUBIOREV.2015.03.008

Feinberg, I., & Campbell, I. G. (2010). Cerebral metabolism and sleep homeostasis: A comment on Vyazovskiy et al. *Brain Research Bulletin*, *81*(1), 1–2. https://doi.org/10.1016/J.BRAINRESBULL.2009.07.017

Field, A. (2013). *Discovering Statistics using IBM SPSS Statistics*. Sage.

Fischl, B., Salat, D. H., Busa, E., Albert, M., Dieterich, M., Haselgrove, C., … Dale, A. M. (2002). Neurotechnique Whole Brain Segmentation: Automated Labeling of Neuroanatomical Structures in the Human Brain. *Neuron*, *33*, 341–355. Retrieved from https://surfer.nmr.mgh.harvard.edu/ftp/articles/fischl02-labeling.pdf

Gaggioni, G., Maquet, P., Schmidt, C., Dijk, D.-J., & Vandewalle, G. (2014). Neuroimaging, cognition, light and circadian rhythms. *Frontiers in Systems Neuroscience*, *8*, 126. https://doi.org/10.3389/fnsys.2014.00126

Govindaiah, G., & Cox, C. L. (2006). Modulation of thalamic neuron excitability by orexins. *Neuropharmacology*, *51*(3), 414–425. https://doi.org/10.1016/j.neuropharm.2006.03.030

Grade, M., Hernandez Tamames, J. A., Pizzini, F. B., Achten, E., Golay, X., & Smits, M. (2015). A neuroradiologist's guide to arterial spin labeling MRI in clinical practice. *Neuroradiology*, *57*(12), 1181–1202. https://doi.org/10.1007/s00234-015-1571-z

Grandner, M. A., Hale, L., Moore, M., & Patel, N. P. (2010). Mortality associated with short sleep duration: The evidence, the possible mechanisms, and the future. *Sleep Medicine*

Reviews, *14*(3), 191–203. https://doi.org/10.1016/j.smrv.2009.07.006

Grivel, J., Cvetkovic, V., Bayer, L., Machard, D., Tobler, I., Mühlethaler, M., & Serafin, M. (2005). The Wake-Promoting Hypocretin/Orexin Neurons Change Their Response to Noradrenaline after Sleep Deprivation. *Journal of Neuroscience*, *25*(16), 4127–4130. https://doi.org/10.1523/JNEUROSCI.0666-05.2005

Guillery, R. W., & Sherman, S. M. (2002). Thalamic Relay Functions and Their Role in Corticocortical Communication: Generalizations from the Visual System. *Neuron*, *33*(2), 163–175. https://doi.org/10.1016/S0896-6273(01)00582-7

Henriksen, O. M., Kruuse, C., Olesen, J., Jensen, L. T., Larsson, H. B., Birk, S., … Rostrup, E. (2013). Sources of variability of resting cerebral blood flow in healthy subjects: A study using 133 Xe SPECT measurements. *Journal of Cerebral Blood Flow and Metabolism*, *33*(5), 787–792. https://doi.org/10.1038/jcbfm.2013.17

Hoddes, E., Zarcone, V., Smythe, H., Phillips, R., & Dement, W. C. (1973). Quantification of Sleepiness: A New Approach. *Psychophysiology*, *10*(4), 431–436. https://doi.org/10.1111/j.1469-8986.1973.tb00801.x

Hodkinson, D. J., O'Daly, O., Zunszain, P. A., Pariante, C. M., Lazurenko, V., Zelaya, F. O., … Williams, S. C. (2014). Circadian and Homeostatic Modulation of Functional Connectivity and Regional Cerebral Blood Flow in Humans under Normal Entrained Conditions. *Journal of Cerebral Blood Flow & Metabolism*, *34*(9), 1493–1499. https://doi.org/10.1038/jcbfm.2014.109

Hodkinson, D. J., O 'daly, O., Zunszain, P. A., Pariante, C. M., Lazurenko, V., Zelaya, F. O., … Williams, S. C. (2014). Circadian and homeostatic modulation of functional connectivity and regional cerebral blood flow in humans under normal entrained conditions. *Journal of Cerebral Blood Flow & Metabolism*, *34109*(10), 1493–1499. https://doi.org/10.1038/jcbfm.2014.109

Horne, J. A., & Ostberg, O. (1976). A self-assessment questionnaire to determine morningness-eveningness in human circadian rhythms. *International Journal of Chronobiology*, *4*(2), 97–110. https://doi:10.1037/t02254-000

Hsieh, K.-C., Gvilia, I., Kumar, S., Uschakov, A., McGinty, D., Alam, M. N., & Szymusiak, R. (2011). c-Fos expression in neurons projecting from the preoptic and lateral

hypothalamic areas to the ventrolateral periaqueductal gray in relation to sleep states. *Neuroscience*, *188*, 55–67. https://doi.org/10.1016/j.neuroscience.2011.05.016

Hsu, D. T., Kirouac, G. J., Zubieta, J.-K., & Bhatnagar, S. (2014). Contributions of the paraventricular thalamic nucleus in the regulation of stress, motivation, and mood. *Frontiers in Behavioral Neuroscience*, *8*, 73. https://doi.org/10.3389/fnbeh.2014.00073

Huber, R., Felice Ghilardi, M., Massimini, M., & Tononi, G. (2004). Local sleep and learning. *Nature*, *430*(6995), 78–81. https://doi.org/10.1038/nature02663

Johns, M. W. (1991). A New Method for Measuring Daytime Sleepiness: The Epworth Sleepiness Scale. *Sleep*, *14*(6), 540–545. https://doi.org/10.1093/sleep/14.6.540

IBM Corp. Released 2017. IBM SPSS Statistics for Windows, Version 25.0. Armonk, NY: IBM Corp

Kasahara, T., Takata, A., Kato, T. M., Kubota-Sakashita, M., Sawada, T., Kakita, A., … Kato, T. (2016). Depression-like episodes in mice harboring mtDNA deletions in paraventricular thalamus. *Molecular Psychiatry*, *21*(1), 39–48. https://doi.org/10.1038/mp.2015.156

Khitrov, M. Y., Laxminarayan, S., Thorsley, D., Ramakrishnan, S., Rajaraman, S., Wesensten, N. J., & Reifman, J. (2014). PC-PVT: A platform for psychomotor vigilance task testing, analysis, and prediction. *Behavior Research Methods*, *46*(1), 140–147. https://doi.org/10.3758/s13428-013-0339-9

Lim, J., & Dinges, D. F. (2008). Sleep deprivation and vigilant attention. In *Annals of the New York Academy of Sciences* (Vol. 1129, pp. 305–322). Blackwell Publishing Inc. https://doi.org/10.1196/annals.1417.002

Lim, J., & Dinges, D. F. (2010). A Meta-Analysis of the Impact of Short-Term Sleep Deprivation on Cognitive Variables. *Psychological Bulletin*, *136*(3), 375–389. https://doi.org/10.1037/a0018883

Lim, J., Wu, W. chau, Wang, J., Detre, J. A., Dinges, D. F., & Rao, H. (2010). Imaging brain fatigue from sustained mental workload: An ASL perfusion study of the time-on-task effect. *NeuroImage*, *49*(4), 3426–3435. https://doi.org/10.1016/j.neuroimage.2009.11.020

Liu, X. G., Zhang, B. J., Xu, X. H., Huang, Z. L., & Qu, W. M. (2012). Lesions of

suprachiasmatic nucleus modify sleep structure but do not alter the total amount of daily sleep in rats. *Sleep and Biological Rhythms*, *10*(4), 293–301. https://doi.org/10.1111/j.1479-8425.2012.00572.x

Longordo, F., Kopp, C., & Lüthi, A. (2009). Consequences of sleep deprivation on neurotransmitter receptor expression and function. *European Journal of Neuroscience*. https://doi.org/10.1111/j.1460-9568.2009.06719.x

Lu, H., Clingman, C., Golay, X., & van Zijl, P. C. M. (2004). Determining the longitudinal relaxation time (T1) of blood at 3.0 Tesla. *Magnetic Resonance in Medicine*, *52*(3), 679–682. https://doi.org/10.1002/mrm.20178

Ma, N., Dinges, D. F., Basner, M., & Rao, H. (2015). How Acute Total Sleep Loss Affects the Attending Brain: A Meta-Analysis of Neuroimaging Studies. *Sleep*, *38*(2), 233–240. https://doi.org/10.5665/sleep.4404

Marino, M., Li, Y., Rueschman, M. N., Winkelman, J. W., Ellenbogen, J. M., Solet, J. M., … Buxton, O. M. (2013). Measuring Sleep: Accuracy, Sensitivity, and Specificity of Wrist Actigraphy Compared to Polysomnography. *Sleep*, *36*(11), 1747–1755. https://doi.org/10.5665/sleep.3142

Martin, J. L., & Hakim, A. D. (2011). Wrist Actigraphy. *Chest*, *139*(6), 1514–1527. https://doi.org/10.1378/chest.10-1872

McClung, C. A. (2007). Circadian genes, rhythms and the biology of mood disorders. *Pharmacology & Therapeutics*, *114*(2), 222–32. https://doi.org/10.1016/j.pharmthera.2007.02.003

Moore, R. Y. (2007). Suprachiasmatic nucleus in sleep-wake regulation. *Sleep Medicine, 8 Suppl 3*, 27–33. https://doi.org/10.1016/j.sleep.2007.10.003

Norskhelseinformatikk. (2015). Beregning av kaloribehov. Retrieved from https://nhi.no/skjema-og-kalkulatorer/kalkulatorer/diverse/beregning-av-kaloribehov/

Ohayon, M. M. (2011). Epidemiological Overview of sleep Disorders in the General Population. *Sleep Med Res*, *2*(1), 1–9. https://doi.org/10.17241/smr.2011.2.1.1

Pallesen, S., Bjorvatn, B., Nordhus, I. H., Sivertsen, B., Hjørnevik, M., & Morin, C. M. (2008). A New Scale for Measuring Insomnia: The Bergen Insomnia Scale. *Perceptual and Motor Skills*, *107*(3), 691–706. https://doi.org/10.2466/pms.107.3.691-706

Paus, T., Zatorre, R. J., Hofle, N., Caramanos, Z., Gotman, J., Petrides, M., & Evans, A. C. (1997). Time-Related Changes in Neural Systems Underlying Attention and Arousal During the Performance of an Auditory Vigilance Task. *Journal of Cognitive Neuroscience*, *9*(3), 392–408. https://doi.org/10.1162/jocn.1997.9.3.392

Pinault, D. (2004). The thalamic reticular nucleus: structure, function and concept. *Brain Research Reviews*, *46*(1), 1–31. https://doi.org/10.1016/j.brainresrev.2004.04.008

Poudel, G. R., Innes, C. R. H., & Jones, R. D. (2012). Cerebral Perfusion Differences Between Drowsy and Nondrowsy Individuals After Acute Sleep Restriction. *Sleep*, *35*(8), 1085–1096. https://doi.org/10.5665/sleep.1994

Raichle, M. E., Grubb, R. L., Gado, M. H., Eichling, J. O., & Ter-Pogossian, M. M. (1976). Correlation Between Regional Cerebral Blood Flow and Oxidative Metabolism. *Archives of Neurology*, *33*(8), 523. https://doi.org/10.1001/archneur.1976.00500080001001

Roth, T., Zammit, G., Kushida, C., Doghramji, K., Mathias, S. D., Wong, J. M., & Buysse, D. J. (2002). A new questionnaire to detect sleep disorders. *Sleep Medicine*, *3*(2), 99–108. https://doi:10.1016/s1389-9457(01)00131-9

Saper, C. B., Fuller, P. M., Pedersen, N. P., Lu, J., & Scammell, T. E. (2010). Sleep State Switching. *Neuron*, *68*(6), 1023–1042. https://doi.org/10.1016/J.NEURON.2010.11.032

Saper, C. B., Lu, J., Chou, T. C., & Gooley, J. (2005, March). The hypothalamic integrator for circadian rhythms. *Trends in Neurosciences*. https://doi.org/10.1016/j.tins.2004.12.009

Saper, C. B., Scammell, T. E., & Lu, J. (2005). Hypothalamic regulation of sleep and circadian rhythms. *Nature*, *437*(7063), 1257–1263. https://doi.org/10.1038/nature04284

Schmidt, C., Collette, F., Leclercq, Y., Sterpenich, V., Vandewalle, G., Berthomier, P., … Peigneux, P. (2009). Homeostatic Sleep Pressure and Responses to Sustained Attention in the Suprachiasmatic Area. *Science*, *324*(5926), 516–519. https://doi.org/10.1126/science.1167337

Schwartz, M. D., & Kilduff, T. S. (2015). The Neurobiology of Sleep and Wakefulness. *Psychiatric Clinics of North America*. https://doi.org/10.1016/j.psc.2015.07.002

Sennels, H. P., Jørgensen, H. L., Hansen, A.-L. S., Goetze, J. P., & Fahrenkrug, J. (2011). Diurnal variation of hematology parameters in healthy young males: The Bispebjerg

study of diurnal variations. *Scandinavian Journal of Clinical and Laboratory Investigation*, *71*(7), 532–541. https://doi.org/10.3109/00365513.2011.602422

Shannon, B. J., Dosenbach, R. A., Su, Y., Vlassenko, A. G., Larson-Prior, L. J., Nolan, T. S., … Raichle, M. E. (2013). Morning-evening variation in human brain metabolism and memory circuits. *Journal of Neurophysiology*, *109*(5), 1444–56. https://doi.org/10.1152/jn.00651.2012

Shao, Y., Wang, L., Ye, E., Jin, X., Ni, W., Yang, Y., … Yang, Z. (2013). Decreased Thalamocortical Functional Connectivity after 36 Hours of Total Sleep Deprivation: Evidence from Resting State fMRI. *PLoS ONE*, *8*(10), e78830. https://doi.org/10.1371/journal.pone.0078830

Sherman, S. M. (2007, August). The thalamus is more than just a relay. *Current Opinion in Neurobiology*. https://doi.org/10.1016/j.conb.2007.07.003

Strecker, R. E., Morairty, S., Thakkar, M. M., Porkka-Heiskanen, T., Basheer, R., Dauphin, L. J., … McCarley, R. W. (2000). Adenosinergic modulation of basal forebrain and preoptic/anterior hypothalamic neuronal activity in the control of behavioral state. *Behavioural Brain Research*, *115*(2), 183–204. https://doi.org/10.1016/S0166-4328(00)00258-8

Taillard, J., Philip, P., Coste, O., Sagaspe, P., & Bioulac, B. (2003). The circadian and homeostatic modulation of sleep pressure during wakefulness differs between morning and evening chronotypes. *Journal of Sleep Research*, *12*(4), 275–82. https://doi:10.1046/j.0962-1105.2003.00369.x

The Mathworks Inc. (2017). Matlab (Version 2017a for Windows), Natick, Massachusetts, United States

Thomas, M. L., Sing, H. C., Belenky, G., Holcomb, H. H., Mayberg, H. S., Dannals, R. F., … Redmond, D. P. (2003). Neural basis of alertness and cognitive performance impairments during sleepiness II. Effects of 48 and 72 h of sleep deprivation on waking human regional brain activity. *Thalamus & Related Systems*, *2*, 199–229. https://doi.org/10.1016/S1472-9288(03)00020-7

Thomas, M., Sing, H., Belenky, G., Holcomb, H., Mayberg, H., Dannals, R., … Redmond, D. (2000). Neural basis of alertness and cognitive performance impairments during sleepiness. I. Effects of 24 h of sleep deprivation on waking human regional brain

activity. *Journal of Sleep Research*, *9*(4), 335–52. https://doi:10.1046/j.1365-2869.2000.00225.x

Tomasi, D., Wang, R. L., Telang, F., Boronikolas, V., Jayne, M. C., Wang, G.-J., … Volkow, N. D. (2009). Impairment of attentional networks after 1 night of sleep deprivation. *Cerebral Cortex*, *19*(1), 233–240. https://doi.org/10.1093/cercor/bhn073

Tononi, G., & Cirelli, C. (2003). Sleep and synaptic homeostasis: a hypothesis. *Brain Research Bulletin*, *62*(2), 143–150. https://doi.org/10.1016/j.brainresbull.2003.09.004

Tononi, G., & Cirelli, C. (2006). Sleep function and synaptic homeostasis. *Sleep Medicine Reviews*, *10*(1), 49–62. https://doi.org/10.1016/j.smrv.2005.05.002

Van der Werf, Y. D., Jolles, J., Witter, M. P., & Uylings, H. B. M. (2003). Contributions of thalamic nuclei to declarative memory functioning. *Cortex; a Journal Devoted to the Study of the Nervous System and Behavior*, *39*(4–5), 1047–62. https://doi:10.1016/s0010-9452(08)70877-3

Van der Werf, Y. D., Witter, M. P., & Groenewegen, H. J. (2002). The intralaminar and midline nuclei of the thalamus. Anatomical and functional evidence for participation in processes of arousal and awareness. *Brain Research. Brain Research Reviews*, *39*(2–3), 107–40. https://doi:10.1016/s0165-0173(02)00181-9

Vyazovskiy, V. V., Cirelli, C., Tononi, G., & Tobler, I. (2008). Cortical metabolic rates as measured by 2-deoxyglucose-uptake are increased after waking and decreased after sleep in mice. *Brain Research Bulletin*, *75*(5), 591–597. https://doi.org/10.1016/j.brainresbull.2007.10.040

Vyazovskiy, V. V., Olcese, U., Hanlon, E. C., Nir, Y., Cirelli, C., & Tononi, G. (2011). Local sleep in awake rats. *Nature*, *472*(7344), 443–447. https://doi.org/10.1038/nature10009

Vyazovskiy, V. V., Tobler, I., Cirelli, C., & Tononi, G. (2009). Author's reply to "Cerebral metabolism and sleep homeostasis: A comment on Vyazovskiy et al." *Brain Research Bulletin*, *80*(6), 443–445. https://doi.org/10.1016/j.brainresbull.2009.08.003

Vyazovskiy, V. V, Cirelli, C., Pfister-Genskow, M., Faraguna, U., & Tononi, G. (2008). Molecular and electrophysiological evidence for net synaptic potentiation in wake and depression in sleep. *Nature Neuroscience*, *11*(2), 200–208. https://doi.org/10.1038/nn2035

Watson, N. F., Badr, M. S., Belenky, G., Bliwise, D. L., Buxton, O. M., Buysse, D., … Tasali, E. (2015). Recommended Amount of Sleep for a Healthy Adult: A Joint Consensus Statement of the American Academy of Sleep Medicine and Sleep Research Society. *SLEEP*, *38*(6), 843–844. https://doi.org/10.5665/sleep.4716

Wolf, E., Kuhn, M., Normann, C., Mainberger, F., Maier, J. G., Maywald, S., … Nissen, C. (2016). Synaptic plasticity model of therapeutic sleep deprivation in major depression. *Sleep Medicine Reviews*, *30*, 53–62. https://doi.org/10.1016/j.smrv.2015.11.003

Wu, J., Buchsbaum, M. S., Gillin, J. C., Tang, C., Cadwell, S., Wiegand, M., … Keator, D. (1999). Prediction of antidepressant effects of sleep deprivation by metabolic rates in the ventral anterior cingulate and medial prefrontal cortex. *The American Journal of Psychiatry*, *156*(8), 1149–58. https://doi.org/10.1176/ajp.156.8.1149

Wu, J. C., Gillin, J. C., Buchsbaum, M. S., Chen, P., Keator, D. B., Khosla Wu, N., … Bunney, W. E. (2006). Frontal lobe metabolic decreases with sleep deprivation not totally reversed by recovery sleep. *Neuropsychopharmacology*, *31*(12), 2783–2792. https://doi.org/10.1038/sj.npp.1301166

Wu, J. C., Gillin, J. C., Buchsbaum, M. S., Hershey, T., Hazlett, E., Sicotte, N., & Bunney, W. E. (1991). The effect of sleep deprivation on cerebral glucose metabolic rate in normal humans assessed with positron emission tomography. *Sleep*, *14*(2), 155–62. https:// doi:10.1093/sleep/14.2.155

Zaharchuk, G. (2014). Arterial spin-labeled perfusion imaging in acute ischemic stroke. *Stroke*, *45*(4), 1202–7. https://doi.org/10.1161/STROKEAHA.113.003612

Zhang, M., Lu, Z., Feng, Q., & Zhang, Y. (2017). Automatic Thalamus Segmentation from Magnetic Resonance Images Using Multiple Atlases Level Set Framework (MALSF). *Scientific Reports*, *7*(1), 4274. https://doi.org/10.1038/s41598-017-04276-6

6. APPENDICES

Appendix 1. Standardized activity plan

På PRISMA

0700-0745:	Fantomscan/QA, klargjøring av magnetrommet
0715-0730:	Klargjøring av SSS & KSS, punching av personalia på scanner
0730:	Møte deltager 1 ved hovedinngangen
0740:	SSS, KSS
0742:	Ta av aktigraf, gjennomgå kontraindikasjon, klargjøre for MR
0745-0815:	MRI1
0800:	Møte deltager 2 ved hovedinngangen
0810:	SSS, KSS
0812:	Ta av aktigraf, gjennomgå kontraindikasjon, klargjøre for MR
0815-0845:	MRI1
0900:	Gå til Gaustad

På Gaustad

0910:	PVT deltager 1 og 2
	Lage frokost
0915:	Frokost med kaffe/te
1000-1030:	SSS & KSS (kl. 10 presis), GSAQ, ESS, Bergen Insomnia, Horne-Østberg, PSQI
1030-1100:	Gjennomgang av søvndagbok deltager 1
	Deltager 2 fritid til skjerm
1100-1110:	PVT deltager 1 og 2
1110-1130:	Gjennomgang av søvndagbok deltager 2
	Deltager 2 fritid til skjerm
1130-1200:	Fritid til skjerm
1200-1205:	SSS, KSS
	Lage mellommåltid/frukt
1205-1215:	Frukt
1215-1300:	Skjermtid
1300-1310:	PVT
1310-1400:	Tur til butikken
1331:	Abstinens koffein

1400-1405:	SSS, KSS
	Lage lunsj
1405-1430:	Lunsj
1430-1500:	Skjermtid
	Rydde bort lunsj og koffein
15:00-15:10:	PVT
1510-1600:	Skjermtid
1600-1605:	SSS, KSS
1602-1700:	Skjermtid
	Begynne på middag (1630-ish)
1700-1710:	PVT
1710-1730:	Middag
1731:	Abstinens nikotin
1730-1800:	Lese, brettspill
1800-1805:	SSS, KSS
1805-1900:	Brettspill, yatzy
1900-1910:	PVT
1910-1920:	Forberede avreise til PRISMA
1920:	Gå til PRISMA

På PRISMA

1915:	Nattevakt ankommer
1915-1930:	Klargjøring av PRISMA
1930-2000:	MRI2 deltager 1
2000-2030:	MRI2 deltager 2
2004-2005:	SSS, KSS deltager 1
2030-2031:	SSS, KSS deltager 2
2045-2055:	Gå til Gaustad med nattevakt
	Dagvakt går hjem

På Gaustad

2100-2110:	PVT
2110-2200:	Skjermtid, kaffe
2200-2205:	SSS, KSS
	Lage kveldsmat

2205-2230: Kveldsmat

2230-2300: Skjermtid

Rydde bort kveldsmat

2300-2310: PVT

2310-0000: Skjermtid

0000-0005: SSS, KSS

0002-0100: Langfilm på storskjerm, del 1 – med snacks

0100-0110: PVT

0110-0200: Langfilm på storskjerm, del 2 – med snacks

0131: Abstinens koffein

0200-0205: SSS, KSS

0205-0230: Spasertur på Gaustad-området

0230-0300: Skjermtid

0300-0310: PVT

Lage måltid

0310-0330: Lett varmt måltid (tomatsuppe)

0330-0400: Skjermtid

04:00-04:05: SSS, KSS

0405-0430: Skjermtid

0430-0500: Spasertur på Gaustad-området

0500-0510: PVT

Lage mellommåltid/frukt

0510-0520: Frukt

0520-0600: Brettspill

0531: Abstinens nikotin

0600-0605: SSS, KSS

0605-0700: Brettspill

0700-0710: PVT

0710-0720: Forberede avreise til PRISMA

0720-0730: Gå til PRISMA

På PRISMA

0650-0700: Dagvakt ankommer

0700-0730: Fantomscan/QA

0730-0800: MRI3 deltager 1

0800-0830: MRI3 deltager 2

0804-0805: SSS, KSS deltager 1

0830-0831: SSS, KSS deltager 2

0845-0855: Spasere til Gaustad

Nattevakt går hjem

På Gaustad

0900-0905: PVT

Lage frokost

0905-0930: Frokost, kaffe

0930-1000: Skjermtid

1000-1001: SSS, KSS

1001: Abstinens koffein

1002-1100: Skjermtid

1100-1110: PVT

1110-1200: Tur til butikken

1200-1205: SSS, KSS

Lage lunsj

1205-1230: Lunsj

1230-1300: Skjermtid

1300-1310: PVT

1310-1330: Spasertur på Gaustad-området

1330-1400: Brettspill eller noe annet interaktivt

1331: Abstinens nikotin

1400-1405: SSS, KSS

1405-1500: Brettspill

1500-1510: PVT

1510-1520: Forberede avreise til PRISMA, pakke sammen ting

1520-1530: Gå til PRISMA

På PRISMA

1515: Nattevakt ankommer

Klargjøring av PRISMA

1530-1600: MRI4 deltager 1

1600-1630: MRI4 deltager 2

1604-1605: SSS, KSS deltager 1

1605-1615: PVT deltager 1

1630-1631: SSS, KSS deltager 2

1631-1636: PVT deltager 2

1645: Deltagere går hjem

Appendix 2. Sleep diary

SLEEP DIARY

Name: Answer question 1 and 2 before bedtime, the rest of the scale in the morning. Remember to note the date.

	Example 01.01.10	Day 1	Day 2	Day 3	Day 4	Day 5	Day 6	Day 7
1. How was your functioning during the day? 1 = very good, 2 good, 3 = average, 4 = bad, 5 = very bad	4							
2. Have you taken one or more naps during the day? Note the time for each nap.	16-16.30 and 18.15-18.30							
3. Have you taken sleep medication and/or alcohol to sleep? Note mediation or type of alcohol and dose	5 mg Imovane 1 glass redwine							
4. When did you go to bed? When did you turn off the light?	22.30 23.00							
5. How long did it take from the light was turned off till you fell asleep?	45 min							
6. How many times did you wake up during the night?	3							
7. How long were the period of awakening (indicate how many minutes per awakening)?	15, 30, 80							
8. When did you wake up in the morning without falling back asleep? Note the time for your final awakening.	06.15							
9. When did you rise?	06.40							
10. How was your last night of sleep in total: 1 = very light, 2 = light, 3 = average, 4 = deep, 5 = very deep.	1							
11. Have you used tobacco during the day? Note type and dose	10 snus							
12. Have you consumed drinks containing caffeine today? Note type and dose.	2 cups of coffee 250ml Red Bull							

Appendix 3. MRI scan protocol

SIEMENS MAGNETOM Prisma

\\IVS\Prosjekter\Cerebrum\Nessun Dorma 2\AAHead_Scout_32ch
TA: 0:14 PM: FIX Voxel size: 1.6×1.6×1.6 mmPAT: 3 Rel. SNR: 1.00 : fl

Properties

Prio recon	Off
Load images to viewer	On
Inline movie	Off
Auto store images	On
Load images to stamp segments	On
Load images to graphic segments	On
Auto open inline display	Off
Auto close inline display	Off
Start measurement without further preparation	On
Wait for user to start	Off
Start measurements	Single measurement

Routine

Slab group	1
Slabs	1
Dist. factor	20 %
Position	L0.0 A10.0 H0.0 mm
Orientation	Sagittal
Phase enc. dir.	A >> P
Phase oversampling	0 %
Slice oversampling	0,0 %
Slices per slab	128
FoV read	260 mm
FoV phase	100,0 %
Slice thickness	1,6 mm
TR	3,15 ms
TE	1,37 ms
Averages	1
Concatenations	1
Filter	Prescan Normalize
Coil elements	HEA;HEP

Contrast - Common

TR	3,15 ms
TE	1,37 ms
Flip angle	8 deg

Contrast - Dynamic

Averages	1
Averaging mode	Short term
Reconstruction	Magnitude
Measurements	1

Resolution - Common

FoV read	260 mm
FoV phase	100,0 %
Slice thickness	1,6 mm
Base resolution	160
Phase resolution	100 %
Slice resolution	69 %
Phase partial Fourier	6/8
Slice partial Fourier	6/8
Trajectory	Cartesian

Resolution - iPAT

PAT mode	GRAPPA
Accel. factor PE	3
Ref. lines PE	24
Accel. factor 3D	1

Resolution - iPAT

Reference scan mode	Integrated

Resolution - Filter Image

Image Filter	Off
Distortion Corr.	Off
Prescan Normalize	On
Unfiltered images	Off
Normalize	Off
B1 filter	Off

Resolution - Filter Rawdata

Raw filter	Off
Elliptical filter	Off

Geometry - Common

Slab group	1
Slabs	1
Dist. factor	20 %
Position	L0.0 A10.0 H0.0 mm
Orientation	Sagittal
Phase enc. dir.	A >> P
Slice oversampling	0,0 %
Slices per slab	128
FoV read	260 mm
FoV phase	100,0 %
Slice thickness	1,6 mm
TR	3,15 ms
Multi-slice mode	Sequential
Series	Ascending
Concatenations	1

Geometry - AutoAlign

Slab group	1
Position	L0.0 A10.0 H0.0 mm
Orientation	Sagittal
Phase enc. dir.	A >> P
Initial Position	Isocenter
L	0,0 mm
P	0,0 mm
H	0,0 mm
Initial Rotation	0,00 deg
Initial Orientation	Transversal

System - Miscellaneous

Positioning mode	FIX
Table position	H
Table position	0 mm
MSMA	S - C - T
Sagittal	R >> L
Coronal	A >> P
Transversal	F >> H
Coil Combine Mode	Adaptive Combine
Save uncombined	Off
Matrix Optimization	Off
Coil Select Mode	Off - AutoCoilSelect

System - Adjustments

B0 Shim mode	Tune up
B1 Shim mode	TrueForm
Adjust with body coil	Off

System - Adjustments

Confirm freq. adjustment	Off
Assume Dominant Fat	Off
Assume Silicone	Off
Adjustment Tolerance	Auto

System - Adjust Volume

Position	Isocenter
Orientation	Transversal
Rotation	0,00 deg
A >> P	263 mm
R >> L	350 mm
F >> H	350 mm
Reset	Off

System - pTx Volumes

B1 Shim mode	TrueForm
Excitation	Non-sel.

System - Tx/Rx

Frequency 1H	123,258986 MHz
Correction factor	1
Gain	Low
Img. Scale Cor.	1,000
Reset	Off
? Ref. amplitude 1H	0,000 V

Physio - PACE

Resp. control	Off
Concatenations	1

Inline - Common

Flip angle	8 deg
Measurements	1
Time to center	6,2 s

Inline - Inline

Subtract	Off
Measurements	1
StdDev	Off
Save original images	On

Inline - MIP

MIP-Sag	Off
MIP-Cor	Off
MIP-Tra	Off
MIP-Time	Off
Save original images	On

Inline - Composing

Distortion Corr.	Off

Inline - MapIt

Save original images	On
MapIt	None
Flip angle	8 deg
Measurements	1
Contrasts	1
TR	3,15 ms
TE	1,37 ms

Sequence - Part 1

Introduction	On
Dimension	3D

Sequence - Part 1

Asymmetric echo	Weak
Contrasts	1
Multi-slice mode	Sequential
Bandwidth	540 Hz/Px

Sequence - Part 2

RF pulse type	Fast
Gradient mode	Normal
Excitation	Non-sel.
RF spoiling	On

Sequence - Assistant

Mode	Off

\\IVS\Prosjekter\Cerebrum\Nessun Dorma 2\TOF_2D_tra

TA: 0:54 PM: REF Voxel size: 0.5×0.5×2.5 mmPAT: 3 Rel. SNR: 1.00 : fl_r

Properties

Prio recon	Off
Load images to viewer	On
Inline movie	Off
Auto store images	On
Load images to stamp segments	On
Load images to graphic segments	Off
Auto open inline display	Off
Auto close inline display	Off
Start measurement without further preparation	Off
Wait for user to start	Off
Start measurements	Single measurement

Routine

Slice group	1
Slices	30
Dist. factor	0,00 %
Position	L2.2 A17.5 F67.8 mm
Orientation	Transversal
Phase enc. dir.	A >> P
AutoAlign	Head > Brain
Phase oversampling	0 %
FoV read	256 mm
FoV phase	97,7 %
Slice thickness	2,5 mm
TR	20,0 ms
TE	4,65 ms
Averages	1
Concatenations	30
Filter	Prescan Normalize, Elliptical filter
Coil elements	HEA;HEP

Contrast - Common

TR	20,0 ms
TE	4,65 ms
TD	0,000 ms
MTC	Off
Flip angle	60 deg
Fat suppr.	None
Water suppr.	None

Contrast - Dynamic

Averages	1
Averaging mode	Short term
Reconstruction	Magnitude
Measurements	1
Multiple series	Each measurement

Resolution - Common

FoV read	256 mm
FoV phase	97,7 %
Slice thickness	2,5 mm
Base resolution	256
Phase resolution	100 %
Phase partial Fourier	6/8
Interpolation	On

Resolution - iPAT

PAT mode	GRAPPA

Resolution - iPAT

Accel. factor PE	3
Ref. lines PE	24
Reference scan mode	Integrated

Resolution - Filter Image

Image Filter	Off
Distortion Corr.	Off
Prescan Normalize	On
Unfiltered images	Off
Normalize	Off
B1 filter	Off

Resolution - Filter Rawdata

Raw filter	Off
Elliptical filter	On
POCS	Off

Geometry - Common

Slice group	1
Slices	30
Dist. factor	0,00 %
Position	L2.2 A17.5 F67.8 mm
Orientation	Transversal
Phase enc. dir.	A >> P
FoV read	256 mm
FoV phase	97,7 %
Slice thickness	2,5 mm
TR	20,0 ms
Multi-slice mode	Sequential
Series	Descending
Concatenations	30

Geometry - AutoAlign

Slice group	1
Position	L2.2 A17.5 F67.8 mm
Orientation	Transversal
Phase enc. dir.	A >> P
AutoAlign	Head > Brain
Initial Position	L2.2 A17.5 F67.8
L	2,2 mm
A	17,5 mm
F	67,8 mm
Initial Rotation	-0,01 deg
Initial Orientation	Transversal

Geometry - Saturation

Fat suppr.	None
Water suppr.	None
Special sat.	Tracking H
Gap	10 mm
Thickness	40 mm

System - Miscellaneous

Positioning mode	REF
Table position	H
Table position	0 mm
MSMA	S - C - T
Sagittal	R >> L
Coronal	A >> P
Transversal	F >> H

System - Miscellaneous

Coil Combine Mode	Sum of Squares
Save uncombined	Off
Matrix Optimization	Off
AutoAlign	Head > Brain
Coil Select Mode	On - AutoCoilSelect

System - Adjustments

B0 Shim mode	Tune up
B1 Shim mode	TrueForm
Adjust with body coil	Off
Confirm freq. adjustment	Off
Assume Dominant Fat	Off
Assume Silicone	Off
Adjustment Tolerance	Auto

System - Adjust Volume

Position	Isocenter
Orientation	Transversal
Rotation	0,00 deg
A >> P	263 mm
R >> L	350 mm
F >> H	350 mm
Reset	Off

System - pTx Volumes

B1 Shim mode	TrueForm

System - Tx/Rx

Frequency 1H	123,258986 MHz
Correction factor	1
Gain	High
Img. Scale Cor.	1,000
Reset	Off
? Ref. amplitude 1H	0,000 V

Physio - Signal1

1st Signal/Mode	None
TR	20,0 ms
Concatenations	30

Physio - Cardiac

Fat suppr.	None
Dark blood	Off
FoV read	256 mm
FoV phase	97,7 %
Phase resolution	100 %

Angio - Common

Flow direction	F >> H
Flip angle	60 deg
MTC	Off
Measurements	1

Angio - Inline

Subtract	Off
Measurements	1
StdDev	Off
Save original images	On

Angio - MIP

MIP-Sag	On
MIP-Cor	On
MIP-Tra	Off

Angio - MIP

MIP-Time	Off
Save original images	On

Angio - Composing

Distortion Corr.	Off

Sequence - Part 1

Introduction	On
Dimension	2D
Asymmetric echo	Allowed
Contrasts	1
Flow comp.	Yes
Multi-slice mode	Sequential
Bandwidth	199 Hz/Px

Sequence - Part 2

Gradient mode	Fast
RF spoiling	On

Sequence - Assistant

Mode	Off

\\IVS\Prosjekter\Cerebrum\Nessun Dorma 2\ASL

TA: 6:58 PM: REF Voxel size: 3.4×3.4×3.4 mmPAT: 3 Rel. SNR: 1.00 : tg818l

Properties

Prio recon	Off
Load images to viewer	On
Inline movie	Off
Auto store images	On
Load images to stamp segments	Off
Load images to graphic segments	Off
Auto open inline display	Off
Auto close inline display	Off
Start measurement without further preparation	Off
Wait for user to start	Off
Start measurements	Single measurement

Routine

Slab group	1
Slabs	1
Dist. factor	50 %
Position	L0.0 A5.3 H11.6 mm
Orientation	T > C1.3
Phase enc. dir.	P >> A
AutoAlign	Head > Brain
Phase oversampling	0 %
Slice oversampling	0,0 %
Slices per slab	42
FoV read	220 mm
FoV phase	100,0 %
Slice thickness	3,40 mm
TR	4430 ms
TE	17,56 ms
Averages	1
Concatenations	1
Filter	Prescan Normalize
Coil elements	HEA;HEP

Contrast - Common

TR	4430 ms
TE	17,56 ms
Flip angle	180 deg
Fat suppr.	Fat sat.

Contrast - Dynamic

Averages	1
Averaging mode	Long term
Reconstruction	Magnitude
Measurements	15
Delay in TR	0 ms
Multiple series	Off

Contrast - ASL

Perfusion mode	PICORE Q2T
Suppression Mode	GRAY-WHITE-STRONG
Quality check	Off
Bolus Duration	1800 ms
Inversion Time	3600 ms
Averaging mode	CONSTANT
Inversion Array Size	1

Resolution - Common

FoV read	220 mm
FoV phase	100,0 %

Resolution - Common

Slice thickness	3,40 mm
Base resolution	64
Phase resolution	98 %
Phase partial Fourier	Off
Slice partial Fourier	Off
Interpolation	Off

Resolution - iPAT

PAT mode	GRAPPA
Accel. factor PE	3
Ref. lines PE	24
Accel. factor 3D	1
Ref. lines 3D	24
Reference scan mode	GRE/separate

Resolution - Filter Image

Distortion Corr.	Off
Prescan Normalize	On

Resolution - Filter Rawdata

Raw filter	Off
Elliptical filter	Off
Hamming	Off

Geometry - Common

Slab group	1
Slabs	1
Dist. factor	50 %
Position	L0.0 A5.3 H11.6 mm
Orientation	T > C1.3
Phase enc. dir.	P >> A
Slice oversampling	0,0 %
Slices per slab	42
FoV read	220 mm
FoV phase	100,0 %
Slice thickness	3,40 mm
TR	4430 ms
Multi-slice mode	Interleaved
Series	Ascending
Concatenations	1

Geometry - AutoAlign

Slab group	1
Position	L0.0 A5.3 H11.6 mm
Orientation	T > C1.3
Phase enc. dir.	P >> A
AutoAlign	Head > Brain
Initial Position	L0.0 A5.3 H11.6
L	0,0 mm
A	5,3 mm
H	11,6 mm
Initial Rotation	-179,99 deg
Initial Orientation	T > C
T > C	1,3
> S	0,0

Geometry - Saturation

Fat suppr.	Fat sat.
Special sat.	Parallel F
Gap	5,0 mm

Geometry - Saturation

Thickness	5 mm

System - Miscellaneous

Positioning mode	REF
Table position	H
Table position	0 mm
MSMA	S - C - T
Sagittal	R >> L
Coronal	A >> P
Transversal	F >> H
Coil Combine Mode	Sum of Squares
Matrix Optimization	Off
AutoAlign	Head > Brain
Coil Select Mode	Default

System - Adjustments

B0 Shim mode	Standard
B1 Shim mode	TrueForm
Adjust with body coil	Off
Confirm freq. adjustment	Off
Assume Dominant Fat	Off
Assume Silicone	Off
Adjustment Tolerance	Auto

System - Adjust Volume

Position	L0.0 A5.3 H11.6 mm
Orientation	T > C1.3
Rotation	-179,99 deg
A >> P	220 mm
R >> L	220 mm
F >> H	143 mm
Reset	Off

System - pTx Volumes

B1 Shim mode	TrueForm

System - Tx/Rx

Frequency 1H	123,258986 MHz
Correction factor	1
Gain	Low
Img. Scale Cor.	5,000
Reset	Off
? Ref. amplitude 1H	0,000 V

Physio - Signal1

1st Signal/Mode	None
TR	4430 ms
Concatenations	1
Segments	3

Sequence - Part 1

Introduction	Off
Dimension	3D
Reordering	Centric
Multi-slice mode	Interleaved
Echo spacing	0,51 ms
Bandwidth	2442 Hz/Px

Sequence - Part 2

EPI factor	21
Segments	3
RF pulse type	Normal
Gradient mode	Fast

Sequence - Part 2

Turbo factor	14

Sequence - Special

Perfusion mode	PCASL
M0 scan mode	On
M0 scan TR	4330 ms
BS DelayAfterNulling	40 ms
BS Suppressed T1	154 ms
Lambda	0,90 mL/g
Labeling efficiency	85,0 %
T1 blood	1650 ms
T1 tissue	1330 ms
PCASL Flip angle	28,0 deg.

\\IVS\Prosjekter\Cerebrum\Nessun Dorma 2\MEMPRAGE

TA: 6:03 PM: REF Voxel size: 1.0×1.0×1.0 mmPAT: 2 Rel. SNR: 1.00 : tfl_me

Properties

Prio recon	Off
Load images to viewer	On
Inline movie	Off
Auto store images	On
Load images to stamp segments	On
Load images to graphic segments	On
Auto open inline display	Off
Auto close inline display	Off
Start measurement without further preparation	Off
Wait for user to start	Off
Start measurements	Single measurement

Routine

Slab group	1
Slabs	1
Dist. factor	50 %
Position	Isocenter
Orientation	Sagittal
Phase enc. dir.	A >> P
AutoAlign	Head > Brain
Phase oversampling	0 %
Slice oversampling	0,0 %
Slices per slab	176
FoV read	256 mm
FoV phase	100,0 %
Slice thickness	1,00 mm
TR	2530,0 ms
TE 1	1,69 ms
TE 2	3,55 ms
TE 3	5,41 ms
TE 4	7,27 ms
Averages	1
Concatenations	1
Filter	Prescan Normalize
Coil elements	HEA;HEP

Contrast - Common

TR	2530,0 ms
TE 1	1,69 ms
TE 2	3,55 ms
TE 3	5,41 ms
TE 4	7,27 ms
Magn. preparation	Non-sel. IR
TI	1100 ms
Flip angle	7,0 deg
Fat suppr.	None
Water suppr.	None

Contrast - Dynamic

Averages	1
Averaging mode	Long term
Reconstruction	Magnitude
Measurements	1
Multiple series	Each measurement

Resolution - Common

FoV read	256 mm
FoV phase	100,0 %
Slice thickness	1,00 mm

Resolution - Common

Base resolution	256
Phase resolution	100 %
Slice resolution	100 %
Phase partial Fourier	Off
Slice partial Fourier	Off
Interpolation	Off

Resolution - iPAT

PAT mode	GRAPPA
Accel. factor PE	2
Ref. lines PE	32
Accel. factor 3D	1
Reference scan mode	Integrated

Resolution - Filter Image

Image Filter	Off
Distortion Corr.	Off
Prescan Normalize	On
Unfiltered images	Off
Normalize	Off
B1 filter	Off

Resolution - Filter Rawdata

Raw filter	Off
Elliptical filter	Off

Geometry - Common

Slab group	1
Slabs	1
Dist. factor	50 %
Position	Isocenter
Orientation	Sagittal
Phase enc. dir.	A >> P
Slice oversampling	0,0 %
Slices per slab	176
FoV read	256 mm
FoV phase	100,0 %
Slice thickness	1,00 mm
TR	2530,0 ms
Multi-slice mode	Single shot
Series	Interleaved
Concatenations	1

Geometry - AutoAlign

Slab group	1
Position	Isocenter
Orientation	Sagittal
Phase enc. dir.	A >> P
AutoAlign	Head > Brain
Initial Position	Isocenter
L	0,0 mm
P	0,0 mm
H	0,0 mm
Initial Rotation	0,00 deg
Initial Orientation	Sagittal

Geometry - Navigator

System - Miscellaneous

Positioning mode	REF

System - Miscellaneous

Table position	H
Table position	0 mm
MSMA	S - C - T
Sagittal	R >> L
Coronal	A >> P
Transversal	F >> H
Coil Combine Mode	Adaptive Combine
Save uncombined	Off
Matrix Optimization	Off
AutoAlign	Head > Brain
Coil Select Mode	Default

System - Adjustments

B0 Shim mode	Standard
B1 Shim mode	TrueForm
Adjust with body coil	Off
Confirm freq. adjustment	Off
Assume Dominant Fat	Off
Assume Silicone	Off
Adjustment Tolerance	Auto

System - Adjust Volume

Position	Isocenter
Orientation	Sagittal
Rotation	0,00 deg
A >> P	256 mm
F >> H	256 mm
R >> L	176 mm
Reset	Off

System - pTx Volumes

B1 Shim mode	TrueForm
Excitation	Non-sel.

System - Tx/Rx

Frequency 1H	123,258986 MHz
Correction factor	1
Gain	Low
Img. Scale Cor.	1,000
Reset	Off
? Ref. amplitude 1H	0,000 V

Physio - Signal1

1st Signal/Mode	None
TR	2530,0 ms
Concatenations	1

Physio - Cardiac

Magn. preparation	Non-sel. IR
TI	1100 ms
Fat suppr.	None
Dark blood	Off
FoV read	256 mm
FoV phase	100,0 %
Phase resolution	100 %

Physio - PACE

Resp. control	Off
Concatenations	1

Inline - Common

Subtract	Off
Measurements	1

Inline - Common

StdDev	Off
Save original images	On

Inline - MIP

MIP-Sag	Off
MIP-Cor	Off
MIP-Tra	Off
MIP-Time	Off
Save original images	On

Inline - Composing

Distortion Corr.	Off

Inline - MapIt

Save original images	On
MapIt	None
Flip angle	7,0 deg
Measurements	1
Contrasts	4
TR	2530,0 ms
TE 1	1,69 ms
TE 2	3,55 ms
TE 3	5,41 ms
TE 4	7,27 ms

Sequence - Part 1

Introduction	On
Dimension	3D
Elliptical scanning	Off
Reordering	Linear
Asymmetric echo	Off
Contrasts	4
Flow comp. 1	No
Multi-slice mode	Single shot
Echo spacing	9,8 ms
Bandwidth 1	650 Hz/Px
Bandwidth 2	650 Hz/Px
Bandwidth 3	650 Hz/Px
Bandwidth 4	650 Hz/Px

Sequence - Part 2

RF pulse type	Fast
Gradient mode	Fast
Excitation	Non-sel.
RF spoiling	On
Incr. Gradient spoiling	Off
Turbo factor	176

Sequence - Special

Readout polarity	Positive
Readout trajectory	Bipolar
Gradient spoiling	Siemens
Gradient moment factor	1
Averaging	RMS

Sequence - Assistant

Mode	Off